

N-(Pyrimidin-2-yl)-1,2,3,4-tetrahydroisoquinolin-6-amine Derivatives as Selective Janus Kinase 2 Inhibitors for the Treatment of Myeloproliferative Neoplasms

Tao Yang,[§] Mengshi Hu,[§] Yong Chen,[§] Mingli Xiang, Minghai Tang, Wenyan Qi, Mingsong Shi, Jun He, Xue Yuan, Chufeng Zhang, Kongjun Liu, Jiewen Li, Zhuang Yang,* and Lijuan Chen*



Cite This: <https://dx.doi.org/10.1021/acs.jmedchem.0c01488>



Read Online

ACCESS |



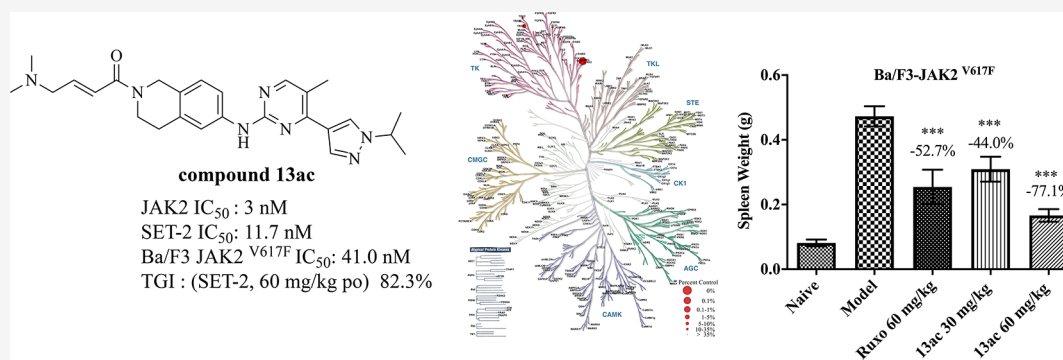
Metrics & More



Article Recommendations



Supporting Information



ABSTRACT: In this study, we described a series of *N*-(pyrimidin-2-yl)-1,2,3,4-tetrahydroisoquinolin-6-amine derivatives as selective JAK2 (Janus kinase 2) inhibitors. Systematic exploration of the structure–activity relationship through cyclization modification based on previously reported compound **18e** led to the discovery of the superior derivative **13ac**. Compound **13ac** showed excellent potency on JAK2 kinase, SET-2, and Ba/F3^{V617F} cells (high expression of JAK2^{V617F} mutation) with IC₅₀ values of 3, 11.7, and 41 nM, respectively. Further mechanistic studies demonstrated that compound **13ac** could downregulate the phosphorylation of downstream proteins of JAK2 kinase in cells. Compound **13ac** also showed good selectivity in kinase scanning and potent in vivo antitumor efficacy with 82.3% tumor growth inhibition in the SET-2 xenograft model. Moreover, **13ac** significantly ameliorated the disease symptoms in a Ba/F3-JAK2^{V617F} allograft model, with 77.1% normalization of spleen weight, which was more potent than Ruxolitinib.

INTRODUCTION

Myeloproliferative neoplasms (MPNs) are a group of malignant bone marrow proliferative diseases originating from hematopoietic stem cells, which manifest as excessive proliferation of one or more lines of myeloid cells.^{1,2} Such diseases include polycythemia vera (PV), essential thrombocythemia (ET), and primary myelofibrosis (PMF), and these diseases can be transformed into each other.³ In myelofibrosis, stem cell transplantation and small molecule therapy are preferred methods of treatment for genetic or clinical high-risk diseases.⁴ The study of MPNs has also facilitated the development of Janus kinase (JAK) inhibitors, such as JAK1/JAK2 inhibitor Ruxolitinib, which has shown promising activity in controlling constitutional symptoms and splenomegaly in MF and PV.^{5,6}

In the JAK kinase family, JAK2 plays a key role in MPNs, especially the JAK2^{V617F} mutation, which is up to 95% in PV and 50% in ET and PMF.^{7–9} The JAK2^{V617F} mutation function has been fully verified, and studies of gene expression profiles have clearly shown that this mutation and the continuously activated

JAK2 signal are present in many MPN patients. This continuous activation leads to malignant cell proliferation and inhibits normal cell apoptosis, thereby causing the occurrence of MPNs.^{10–14} Because of the vital function of JAK2 in MPNs, another JAK2 inhibitor Fedratinib was approved to treat myelofibrosis (MF) in 2019.^{15,16} Several other JAK2 inhibitors with varying degrees of selectivity are in mid to late-stage clinical trials for MF such as Lestaurtinib (CEP701), Momelotinib (CYT-387), Gandotinib (LY2784544), and Pacritinib.^{17–22} Although these drugs have shown excellent disease modification, they all exhibited more or less side effects especially Fedratinib, which was given a “black box warning” on the risk of serious and

Received: August 26, 2020

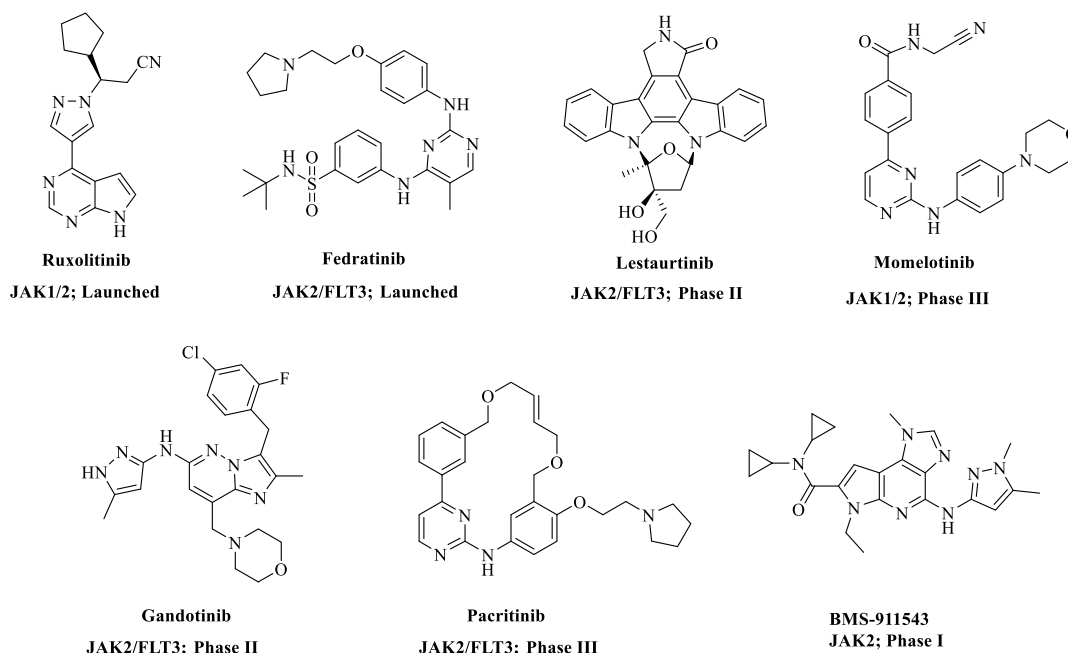


Figure 1. Representative drugs in clinical trials or launched JAK2 inhibitors.

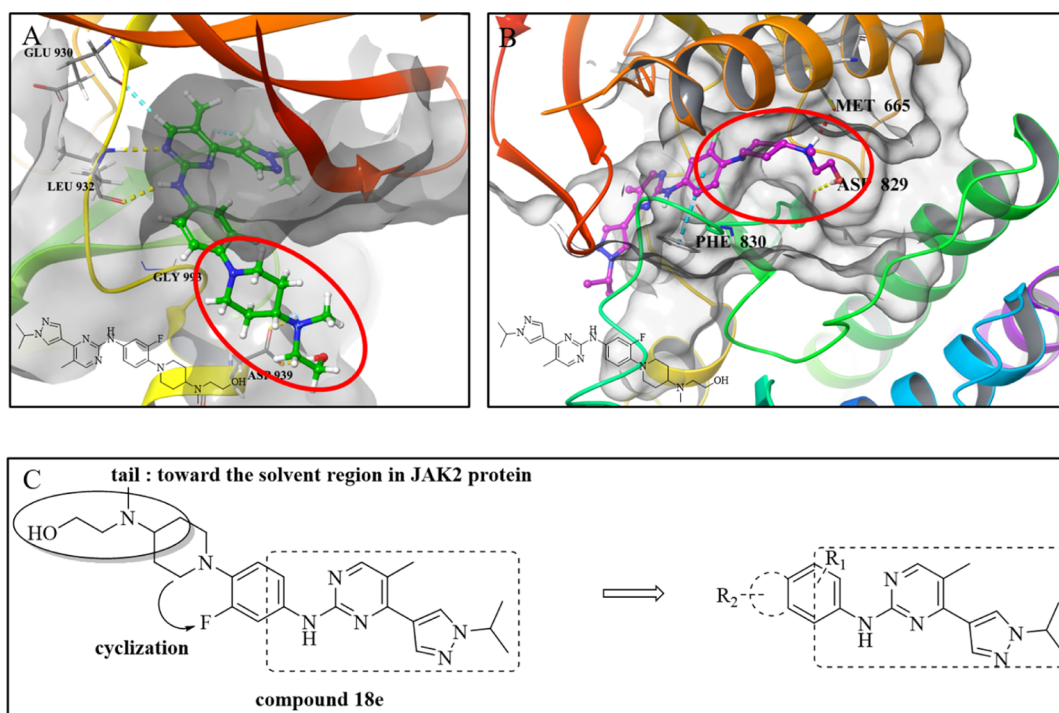


Figure 2. (A) Docking results of **18e** in the JAK2 protein (PDB code: 2XA4); (B) Docking results of **18e** in the FLT3 protein (PDB code: 4RT7); (C) Modifying plans for newly designed compounds.

fatal encephalopathy by the FDA.²³ The side effects may be caused by multitarget activity. Therefore, the development of novel selective JAK2 inhibitors was in need, such as the prospective candidate BMS-911543 (Figure 1).²⁴

In our previous studies, we reported a dual JAK2/FLT3 kinase inhibitor **18e**. The 2-aminopyrimidine scaffold provided a novel hinge binding motif for the design of small-molecular ATP-competitive JAK2/FLT3 inhibitors.²⁵ We analyzed the crystal structure and docking data of **18e** and found that the aminopiperidine tail formed hydrogen bonds with receptor

residues such as Met665 and Asp829, which played a vital role in interaction with FLT3 protein while the tail was exposed to the solvent region in the JAK2-binding pocket (Figure 2A,B). We hypothesized that the modification of the tail might provide a solution to reduce the binding activity for FLT3 but retain the activity for JAK2. Cyclization is a commonly used method in drug design to improve selectivity, such as the broad-spectrum anticancer drug Repotrectinib, Larotrectinib, and the fourth generation EGFR inhibitor BI-4020.^{26–28} Therefore, our group considered cyclizing the tail and modifying the newly formed

ring with various substituents to improve the JAK2 selectivity and activity (Figure 2C). In this article, we described our efforts toward identifying potent, selective JAK2 inhibitors for the treatment of MPNs.

RESULTS AND DISCUSSION

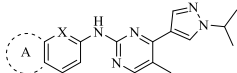
In Vitro Structure–Activity Analysis. Our initial SAR efforts were directed toward cyclizing the tail to retain JAK2 potency and reduce FLT3 potency. SET-2 and Ba/F3 JAK2^{V617F} cells, which overexpressed JAK2^{V617F}, were chosen to determine the JAK2 potency. For FLT3, the activity against MOLM-13, which represents a human acute myeloid leukemia (AML) cell line harboring FLT3 internal tandem duplication (FLT3-ITD), was detected.²⁹ At first, analogs containing four kinds of rings with active substituents hydroxyethyl and hydroxypropyl were synthesized.²⁵ As illustrated in Table 1, 5,6,7,8-tetrahydro-1,6-

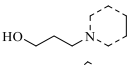
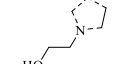
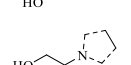
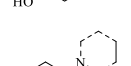
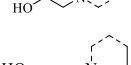
As shown in Table 2, when R¹ was substituted by F, the activity of compounds 13f, 13i, and 13l–13n against JAK2 slightly decreased while the FLT3 potency was increased apparently. We thought that the electron-withdrawing effect of F might enhance the interaction between the amino acid residue and pyrimidine amine, which resulted in an increase in the activity for JAK2 and FLT3. However, the effect of F went against selectivity of JAK2 versus FLT3. Furthermore, the F atom introduced into the benzene at R² position (13k) caused apparent loss of activity both on JAK2 and FLT3. Compounds with a rigid urea bond (13g, 13h, and 13j) reduced the activity toward JAK2 and FLT3 sharply, which indicated the R³ substituent played a key role in activity and selectivity. Among these compounds, 13d and 13e showed the most potent cellular activity and acceptable selectivity, but the cellular activity on the JAK2 related cell lines was still unsatisfactory. Accordingly, based on 1,2,3,4-tetrahydro-isoquinolin, a series of substituents at the R³ position were modified for exploring a more effective and selective compound.

In the previous research, compounds 13d and 13e showed selectivity for FLT3, therefore, hydrophilic saturated alkane substituents with different chain length were introduced to the R³ position (13o–13p). As shown in Table 3, the selectivity and cellular activity of these two compounds did not improve with the increase of the chain length. Comparison of the structures of 13q and 13r suggested that the terminal heteroatom played a certain role in maintaining the activity. Inspired by this result, the heteroatom substituent cyano was introduced to the same position and resulted in a significant improvement in cellular activity and an 8.8-fold increase in selectivity (13t). Subsequently, we extended the cyano chain to obtain compound 13u, and the activity against JAK-related cells decreased. Considering that the cyano group is an unsaturated bond, some other unsaturated groups were also introduced to the R³ position. Obviously, rigid unsaturated substituents had no positive effect on activity enhancement (13s, 13v, and 13w). We further analyzed the cyano group and realized the cyano group possessed potential of hydrolyzing to carboxyl, thus, the carboxyl derivatives were synthesized. Compared to 13y, 13x showed more excellent activity and about 35-fold selectivity for FLT3, which indicated the importance of the double bond. This conclusion was also confirmed by the two groups of compounds 13aa and 13ab and 13ac and 13ad. As compound 13x possessed good activity, we further investigated the conjugated structure by replacing with a larger conjugate system (13z, 13aa). Obviously, the large conjugated system contributed to selectivity and activity. Both carbonyl and amino groups contributed electron-donating effects in the formation of hydrogen bonds, therefore, the benzoyl was replaced by dimethylaminoethyl (13ac). Not surprisingly, compound 13ac also showed potent activity and 75.2-fold selectivity for FLT3. In view of the metabolic instability of the ester bond of compound 13x, the ester bond was replaced with a more stable amide bond (13ae–13ah). However, the activities of these compounds were reduced to certain degrees. So far, we had obtained a number of compounds with excellent cellular activity and acceptable selectivity, occasionally, during the synthetic preparation process, we found that the 6- and 7-amino groups of tetrahydroisoquinoline were similar in space. Hence, the 7-amino tetrahydroisoquinoline analogues were also synthesized on the basis of the earlier active substituent.

As shown in Table 4, most of the newly synthesized compounds (13ai–13ak) exhibited excellent cellular activity

Table 1. Structures and In Vitro Biological Activities of Compounds 13a–e

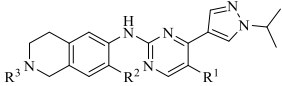


Compd	Substituents		IC ₅₀ (μM) ^a		MOLM-13	SI ^b	% control @100 nM ^c
	X	A	SET-2	Ba/F3 JAK2 ^{V617F}			
13a	N		2.18 ± 0.96	1.43 ± 0.45	2.57 ± 0.34	1.1	88
13b	C		3.79 ± 0.12	4.39 ± 1.9	2.06 ± 0.76	0.54	79
13c	C		0.692 ± 0.19	2.33 ± 0.95	1.78 ± 0.66	2.6	67
13d	C		0.323 ± 0.045	0.431 ± 0.016	1.26 ± 0.15	3.9	66
13e	C		0.394 ± 0.023	0.365 ± 0.052	1.32 ± 0.19	3.4	62
18e			0.270 ± 0.034	0.145 ± 0.050	0.072 ± 0.063	0.27	5

^aIC₅₀ = compound concentration required to inhibit tumor cell proliferation by 50%; data are expressed as the mean ± SEM from the dose–response curves of at least three independent experiments. ^bSI = selectivity index (IC₅₀ (MOLM-13)/IC₅₀ (SET-2)), which represents the selectivity for JAK2 on cells. ^c% control = kinase activity remained.

phthiridine (13a), isoindoline (13b), indoline (13c), and 1,2,3,4-tetrahydro-isoquinolin (13d–13e) all showed obviously weak potency on FLT3, however, the JAK2 potency also decreased apparently except for compounds 13d and 13e. Compared to compound 18e, 13d–13e demonstrated a similar inhibition for JAK2 and poorer activity for FLT3. We speculated that the small ring of 13b and 13c limited the conformation of the substituent, which resulted in poor interactions with the amino acid residue. Because 1,2,3,4-tetrahydro-isoquinolin exhibited desirable selectivity, it was selected as a skeleton. Next, we further examined the effects of substituents around the skeleton.

Table 2. Structures and In Vitro Biological Activities of Compounds 13f–n



Compd	Substituents			IC ₅₀ (μM) ^a				% control @100 nM ^c
	R ¹	R ²	R ³	SET-2	Ba/F3 JAK2 ^{V617F}	MOLM-13	SI ^b	
13f	F	H		0.574 ± 0.13	0.679 ± 0.23	0.453 ± 0.032	0.79	39
13g	Me	H		3.45 ± 1.9	2.18 ± 0.90	2.07 ± 0.32	0.60	99
13h	Me	H		2.35 ± 1.1	1.89 ± 0.98	1.07 ± 0.056	0.45	ND ^d
13i	F	H		0.311 ± 0.26	0.392 ± 0.27	0.453 ± 0.032	1.4	44
13j	Me	H		1.76 ± 0.23	1.21 ± 0.78	2.07 ± 0.29	1.2	ND
13k	Me	F		4.46 ± 1.5	2.57 ± 1.05	> 5	> 1.2	ND
13l	F	H		0.651 ± 0.034	0.760 ± 0.015	0.547 ± 0.125	0.84	43
13m	F	H		0.604 ± 0.13	0.445 ± 0.13	0.455 ± 0.112	0.75	39
13n	F	H		0.492 ± 0.24	0.420 ± 0.31	0.353 ± 0.016	0.72	42

^aIC₅₀ = compound concentration required to inhibit tumor cell proliferation by 50%; data are expressed as the mean ± SEM from the dose–response curves of at least three independent experiments. ^bSI = selectivity index (IC₅₀ (MOLM-13)/IC₅₀ (SET-2)), which represents the selectivity for JAK2 on cells. ^c% control = kinase activity remained. ^d= no detected.

for JAK2 but demonstrated decreased selectivity for FLT3. These results also indicated the spatial position of the substituent had a certain influence on the selectivity. Consideration of the structure novelty, compounds (13t, 13x, 13z, 13aa, 13ac, 13aj, 13al, and 13am) with excellent cellular activity and selectivity were selected for the next kinase selectivity screening.

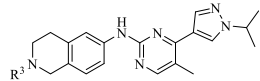
To test the potency of these compounds for JAK2 and FLT3, kinase assays were conducted by Eurofins Discovery. Because of the high homology of the JAK family, it was thought to be selective when the selectivity was greater than 10-fold. As shown in Table 5, compounds 13x, 13aa, 13ac, and 13al exhibited relative selectivity for JAK2. Ruxolitinib, as the first marketed drug for the treatment of myelofibrosis, has varying degrees of damage to the blood cell reduction.³⁰ Another marketed drug Fedratinib showed obvious damage on liver and spleen.³¹ Therefore, safety is an important factor in the development of myelofibrosis drugs. The above-mentioned four compounds all had good performance on cellular and enzymatic selectivity, so we tested their toxicity on a series of normal cells. As shown in Table 6, in comparison with other compounds, 13ac was relatively safe on a panel of normal cells especially normal liver cell. At the same time, after continuous oral administration of 30 and 60 mg/kg of 13ac for 14 days, the routine blood test was conducted (Figure S5), compound 13ac only showed a slight effect on the hematocrit (HCT %) compared to normal mice. This result was consistent with in vitro cell safety screening, and

both proved that 13ac was relatively safe. Based on the above experimental results, 13ac was chosen for further study.

Kinase Selectivity Profiling of 13ac. To further investigate the kinase selectivity of 13ac, its kinome selectivity profile was then examined with Kinase Profile technology developed by Eurofins Discovery. A panel of 361 kinases was tested at a 0.1 μM concentration of 13ac (Table S1). The kinome screening revealed that 13ac exhibited expected selectivity for JAK2 within the human kinome. In addition to high activity on JAK2, 13ac also demonstrated activity against TrkA (Figure 3). TrkA belongs to a subfamily of receptor tyrosine kinases, which is activated by phosphorylation of specific tyrosine sites through dimerization, subsequently, in turn activates downstream signaling pathways, including Ras/MAPK, PI3K/AKT, and PLCγ pathways.^{32,33} These signaling pathways are consistent with JAK2's downstream signaling pathways, besides, patients with MPNs can secondary activate downstream pathways such as PI3K and MAPK via the JAK-STAT signaling pathway, there may be a certain synergy between JAK2 and TrkA for treating MPNs, and the follow-up process was still being conducted.³⁴ Overall, 13ac was relatively selective for JAK2.

Pharmacokinetics of 13ac in Rats. In vitro screening indicated that compound 13ac was a potential JAK2 inhibitor, subsequently, the pharmacokinetic study was conducted. In vitro liver microsomal metabolism showed that *T*_{1/2} of 13ac was 54.6 min, and the in vitro clearance rate was 25.4 L/h/kg, which

Table 3. Structures and In Vitro Biological Activities of Compounds 13o–13h

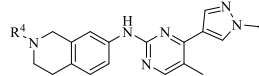


Compd	Substituents R ³	IC ₅₀ ± SEM (μM) ^a			SI ^b	FLT3	% control @100 nM ^c
		SET-2	Ba/F3 JAK2 ^{V617F}	MOLM-13			
13o		0.268 ± 0.034	0.234 ± 0.098	0.879 ± 0.013	3.3	56	
13p		0.312 ± 0.023	0.354 ± 0.005	0.965 ± 0.025	3.1	63	
13q		0.339 ± 0.056	0.302 ± 0.011	0.568 ± 0.101	1.7	40	
13r		0.592 ± 0.032	0.640 ± 0.051	0.754 ± 0.097	1.3	57	
13s		0.288 ± 0.034	0.452 ± 0.018	0.868 ± 0.101	3.0	67	
13t		0.0732 ± 0.0012	0.0578 ± 0.0064	0.647 ± 0.089	8.8	50	
13u		0.296 ± 0.0045	0.177 ± 0.056	0.356 ± 0.125	1.2	35	
13v		0.382 ± 0.067	0.695 ± 0.012	1.48 ± 0.125	3.9	79	
13w		0.794 ± 0.005	0.908 ± 0.0022	1.56 ± 0.345	2.0	85	
13x		0.0137 ± 0.016	0.0103 ± 0.0089	0.497 ± 0.068	36.3	53	
13y		1.04 ± 0.016	0.938 ± 0.23	1.29 ± 0.23	1.2	ND ^d	
13z		0.0521 ± 0.0045	0.010 ± 0.0011	0.458 ± 0.023	8.8	41	
13aa		0.0147 ± 0.0026	0.0128 ± 0.0005	0.758 ± 0.043	51.6	55	
13ab		0.626 ± 0.023	0.784 ± 0.0032	1.055 ± 0.17	1.7	ND	
13ac		0.0117 ± 0.0023	0.0410 ± 0.002	0.880 ± 0.132	75.2	54	
13ad		0.985 ± 0.10	2.48 ± 1.1	1.48 ± 0.72	1.5	ND	
13ae		0.334 ± 0.011	0.128 ± 0.015	0.845 ± 0.046	2.5	78	
13af		0.554 ± 0.015	1.20 ± 0.12	2.09 ± 0.52	3.8	ND	
13ag		0.612 ± 0.0032	0.145 ± 0.032	1.055 ± 0.23	1.7	ND	
13ah		0.329 ± 0.003	0.287 ± 0.011	0.656 ± 0.058	2.0	66	

Table 3. continued

^aIC₅₀ = compound concentration required to inhibit tumor cell proliferation by 50%; data are expressed as the mean ± SEM from the dose–response curves of at least three independent experiments. ^bSI = selectivity index (IC₅₀ (MOLM-13)/IC₅₀ (SET-2)), which represents the selectivity for JAK2 on cells. ^c% control = kinase activity remained. ^d= no detected.

Table 4. Structures and In Vitro Biological Activities of Compounds 13ai–am



Compd	Substituents R ⁴	IC ₅₀ ± SEM (μM) ^a			SI ^b	FLT3	% control @100 nM ^c
		SET-2	Ba/F3 JAK2 ^{V617F}	MOLM-13			
13ai		0.0946 ± 0.003	0.0755 ± 0.0032	0.425 ± 0.120	4.5	51	
13aj		0.0427 ± 0.002	0.0612 ± 0.0011	0.535 ± 0.105	12.5	47	
13ak		0.072 ± 0.005	0.120 ± 0.0053	0.430 ± 0.098	6.0	43	
13al		0.0250 ± 0.0031	0.0505 ± 0.019	0.629 ± 0.057	25.2	59	
13am		0.0153 ± 0.0022	0.0245 ± 0.032	0.456 ± 0.063	29.8	52	

^aIC₅₀ = compound concentration required to inhibit tumor cell proliferation by 50%; data are expressed as the mean ± SEM from the dose–response curves of at least three independent experiments. ^bSI = selectivity index (IC₅₀ (MOLM-13)/IC₅₀ (SET-2)), which represents the selectivity for JAK2 on cells. ^c% control = kinase activity remained.

indicated the potential druggability of 13ac. Therefore, in vivo studies were also performed. The PK properties of 13ac are summarized in Table 7. In rats, 13ac showed fast absorption ($T_{\max} = 0.9$ h), with a peak concentration of 51.1 ng/mL, an AUC of 253.6 ng h/mL, and a terminal half-life of ~1.8 h following a single oral dose of 5 mg/kg. The oral bioavailability of 13ac in rat was 25.7%.

In Vivo Xenograft and Allograft Model Experiments.

As compound 13ac showed acceptable pharmacokinetic properties and excellent activity and kinase selectivity in vitro, the efficacy of 13ac in vivo was tested in the SET-2 cell-inoculated xenograft NOD/SCID mouse models. The average tumor volume at the start was 163.8 mm³, mice were dosed orally daily for 16 days with three doses of 13ac. In comparison with Ruxolitinib, 13ac exhibited a significant tumor growth inhibition of 82.3% without obvious weight change (Table 8, Figures 4A and S6A). After termination of the treatment, tumor growth was measured up to day 36. All mice in the control group died at the 20th day, while only one mouse died in the treatment group after 36 days (Figure 4C). The survival time of mice was improved, which indicated the relative safety and effectiveness of 13ac.

In order to further verify the antitumor effect of 13ac in vivo, a Ba/F3-JAK2^{V617F} allograft model by tail vein injection was established (detailed experiment method shown in Supporting Information). The Ba/F3-JAK2^{V617F} mouse allograft represents a model for a JAK2-driven disease exhibiting hallmark symptoms

Table 5. Kinome Activity and Selectivity of the Preferred Compounds

compd	kinase IC ₅₀ (nM) ^a								
	13t	13x	13z	13aa	13ac	13aj	13al	13am	
kinase subtype	JAK1	43	26	47	60	42	30	24	91
	JAK2	7	2	10	3	3	2	0.9	9
	JAK3	54	77	120	50	94	89	28	147
	TYK2	56	88	79	100	75	52	30	45
	FLT3	108	23	34	30	62	16	18	23
selectivity (folds)	JAK2/JAK1	6.1	13	4.7	20	14	15	26.6	10
	JAK2/JAK3	7.7	38.5	12	16.6	31	44.5	31	16
	JAK2/TYK2	8.0	44	7.9	33.3	25	26	33	5.0
	JAK2/FLT3	15.4	11.5	3.4	10	20.7	8	20	2.5

^aThe biochemical tests were provided by Eurofins Discovery. All data were obtained by double testing.

Table 6. Inhibition of Cellular Proliferation in Normal Cell Lines by Preferred Compounds

cell line	cell type	growth inhibition, IC ₅₀ (μM) ^a			
		13x	13aa	13ac	13al
Vero	African green monkey kidney cell	2.23 ± 0.45	1.05 ± 0.52	6.75 ± 0.28	2.47 ± 0.48
H9c2 (2-1)	rat cardiomyocyte	2.89 ± 0.13	1.43 ± 0.32	6.93 ± 0.18	1.69 ± 0.16
LO2	human normal liver cell	1.53 ± 0.22	2.66 ± 0.11	7.22 ± 0.41	2.03 ± 0.15

^aIC₅₀ = compound concentration required to inhibit tumor cell proliferation by 50%; data are expressed as the mean ± SEM from the dose–response curves of at least three independent experiments.

of myeloproliferative diseases such as splenomegaly and hepatomegaly. In this model, murine Ba/F3-JAK2^{V617F} cells were engrafted by tail vein injection. Treatment with **13ac** at doses of 30 and 60 mg/kg p.o. q.d. was started 4 days after cell inoculation for 20 consecutive days. Ruxolitinib was chosen as a positive control. At the study end, model mice exhibited splenomegaly and hepatomegaly (~5.9-fold and 1.5-fold, respectively). Compound **13ac** treatment at 30 mg/kg p.o. q.d. significantly ameliorated the disease symptoms. Compared to Ruxolitinib, at a dose of 60 mg/kg, **13ac** showed a superior treatment effect with 77.1% normalization of spleen weight (Figures 4D,E and S6D).

Molecular Docking Study of 13ac. The screening results at the cell and kinase levels indicated our previous hypothesis, modification of the tail of lead compound **18e** retained the activity for JAK2 but reduced the potency for FLT3. Further in vivo study indicated the effectiveness in mice. In order to explore the protein-binding mode of **13ac**, the crystal structure of the protein kinase domain of JAK2 from the Protein Data Bank (PDB code: 2XA4) was selected as the docking model.^{35,36} The docking results are presented in Figure 5 (see docking methods in Supporting Information).^{37–42} As demonstrated, the newly synthesized cycle was still toward outside the binding pocket, the reasonable conformation of the **13ac**–JAK2 complex suggested that the pyrimidine amino and one nitrogen atom pyrimidine formed two strong hydrogen bonds with the Leu932 in the distance of acceptor–donor of 2.98 and 3.06 Å. The pyrazole region also connected with Val863, Lys882, Val911, Met929, Leu983, Gly993, and Asp994 with hydrophobic interaction. Meanwhile, the pyrimidine ring formed arene-*H* interaction with Leu983 and Gly935 at the same time. Simultaneously, the terminal amine of the isoquinoline exposed in the solvent formed unexpected electrostatic interaction with Asp939, which might increase the binding activity. Those interactions suggested that **13ac** possessed a good affinity for JAK2 protein.

Cell Cycle Analysis and Apoptosis Assays in SET-2 Cells. JAK2 plays a vital role in cell proliferation and survival; therefore, we examined the effect of **13ac** on the cell cycle. The

experimental results showed that **13ac** induced cell arrest in the G0/G1 phase in a concentration-dependent manner (Figure 6A). A flow cytometry assay was also performed to examine cell apoptosis upon treatment with compound **13ac**. Compound **13ac** induced apoptosis in SET-2 cells in a similar pattern (Figure 6B). At a concentration of 0.80 μM, an apoptosis rate of 49.3% was observed.

Signaling Inhibition of 13ac in JAK2^{V617F}-Expressing Cell Lines and Spleen Lysates. In order to investigate whether the excellent enzymatic activity of compound **13ac** regulates the JAK2 signaling pathway, the phosphorylation status of JAK2 and downstream substrates was detected by Western blot analysis of JAK2^{V617F}-expressing cell lines. After a 2 h treatment with increasing concentrations of compound **13ac**, SET-2 and Ba/F3-JAK2^{V617F} cells were harvested and lysed for an IP/wt assay. As shown in Figure 7A, compound **13ac** inhibited JAK2 and STAT5 phosphorylation in a dose-dependent manner. To explore the selectivity of **13ac** in the signaling pathway, FLT3 and downstream signaling protein AKT were detected.²⁹ Compared to JAK2, poorer inhibition of phosphorylated FLT3 and AKT indicated the selectivity of **13ac**. Selectivity is reflected not only in the kinase level for different subtypes, but also in the downstream effector molecules in the signaling pathway. The analysis for STAT of different subtypes was conducted on the Ba/F3 JAK2^{V617F} cell. As illustrated in Figure 7B, compound **13ac** reduced STAT5 phosphorylation at a concentration of 50 nM while barely showed obvious inhibition for other STAT subtypes even at a concentration of 1000 nM. Furthermore, considering the excellent efficacy of **13ac** in vivo, we also investigated the influence of **13ac** on the JAK2 signaling pathway on the spleen tissue. On day 25, mice were killed and tumor lysates were analyzed for JAK2 signaling by Western blot. As shown in Figure 7C, **13ac** demonstrated a full inhibition of STAT5 phosphorylation.

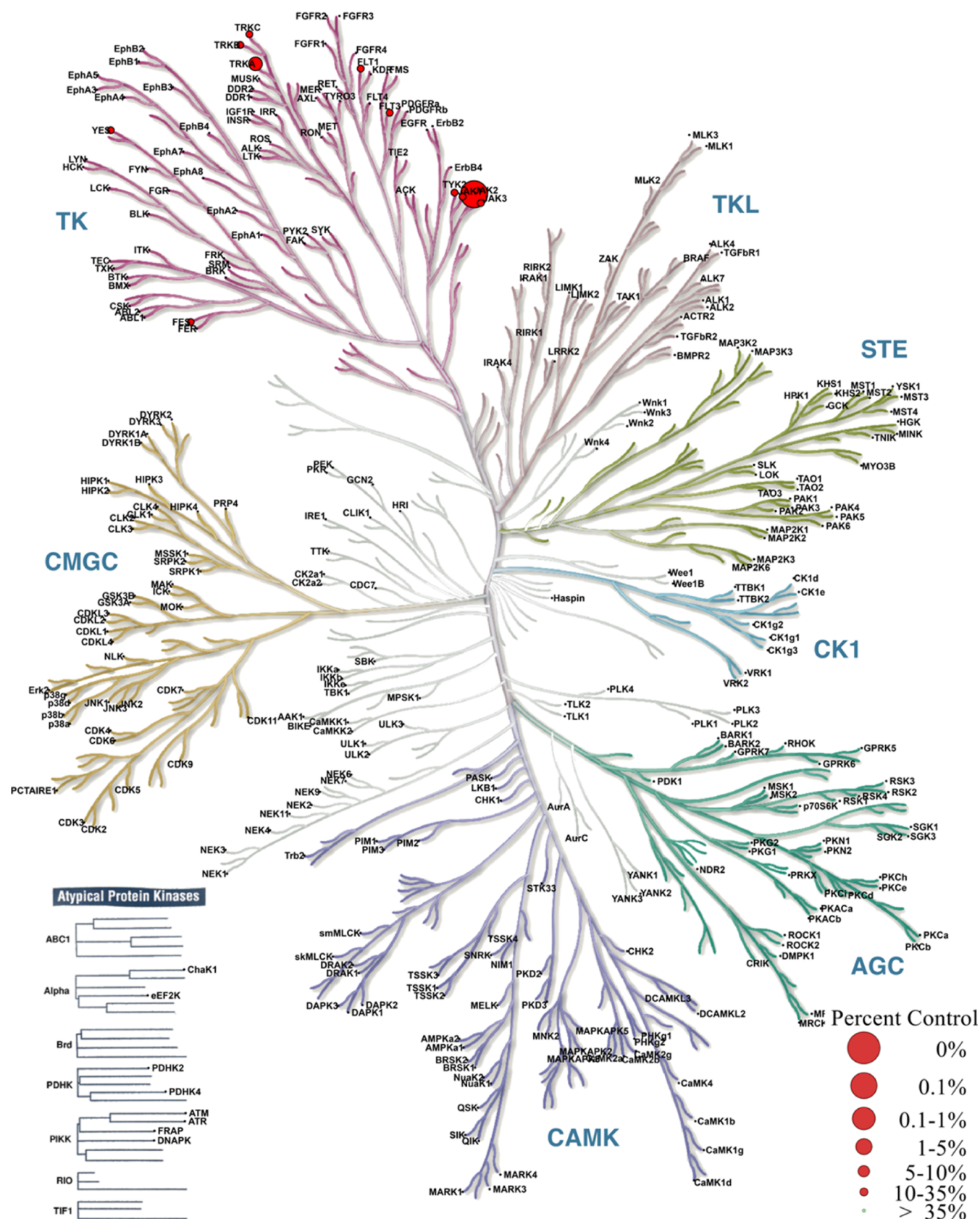


Figure 3. Kinome-wide selectivity profiling of compound 13ac with the Kinase Profile assay by Eurofins Discovery. Measurements were performed at a concentration of 0.1 μ M of the inhibitor in duplicate. The % control means remaining active kinase percentage. The affinity was defined with respect to a dimethyl sulfoxide (DMSO) control. The TREEspot image was mapped with the KinMap software tool provided by Cell Signaling Technology, Inc. (www.cellsignal.com).

Table 7. In Vivo Profiling of Compound 13ac

compd	administration (5 mg/kg)	ADME parameter ^a					F %
		C _{max} (ng/mL)	T _{max} (h)	T _{1/2} (h)	Cl _z (L/h/kg)	AUC _{0-t} (ng·h/mL)	
13ac	oral	51.1 ± 26.5	0.9 ± 0.4	1.8 ± 0.5	28.8 ± 9.5	253.6 ± 24.1	25.7
	intravenous	479.3 ± 28.3	0.08	4.0 ± 1.1	5.01 ± 0.71	987.9 ± 110.2	

^aSprague-Dawley rats (*n* = 5) were treated with solution (2% ethanol and 1% tween 80, pH5) at a dose of 5 mg/kg.

Table 8. Summary of Tumor Growth Inhibition of Compound 13ac

compd	tumor model	administration			survivors	inhibition rate (%)
		schedule ^a	route	dose (mg/kg)		
13ac	SET-2	QD × 16	P.O	15	5/5	51.4
				30		67.8
				60		82.3
				60		52.8
Ruxolitinib				60		52.8

^aQD, every day.

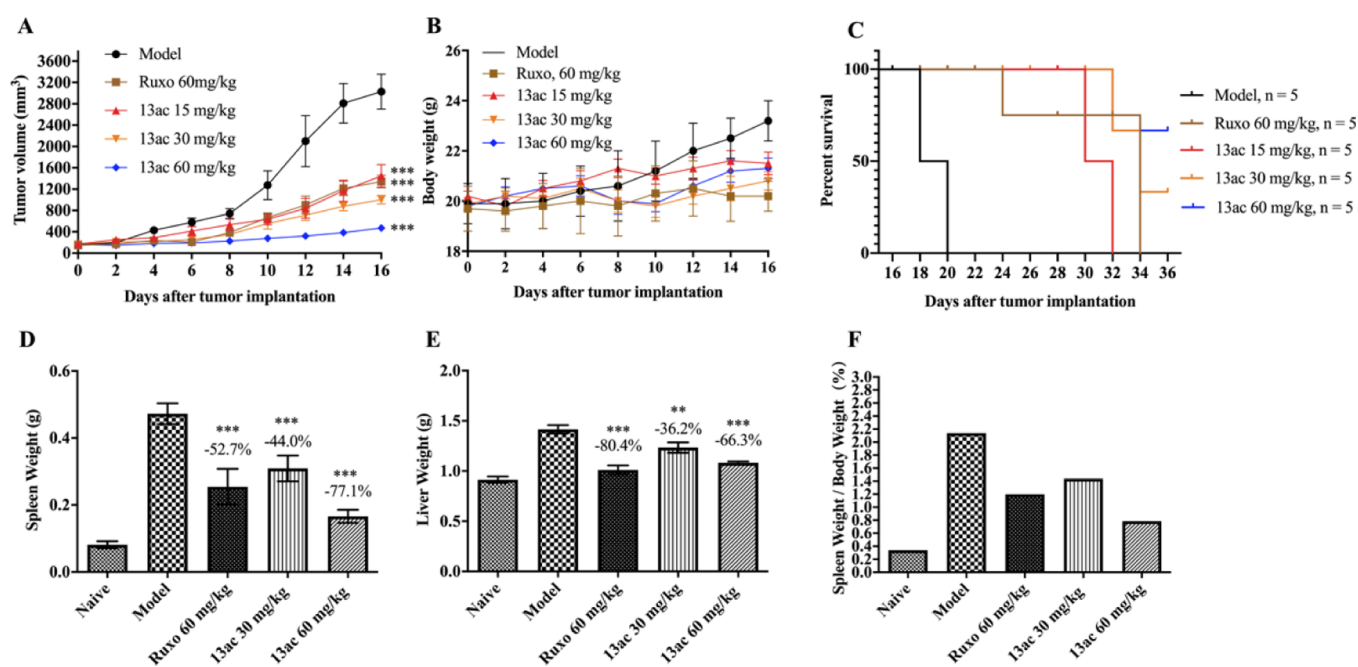


Figure 4. (A) NOD/SCID mice bearing SET-2 tumors (*n* = 5) were treated for 16 consecutive days with 15, 30, and 60 mg/kg 13ac p.o. q.d. Tumor volumes were measured every two days. ***, *P* < 0.01 ANOVA, Dunnett's post test; (B) body weight change in SET-2 cell-inoculated xenograft NOD/SCID mouse models; (C) NOD/SCID mice bearing SET-2 tumors (*n* = 5) were treated for 36 consecutive days with 15, 30, and 60 mg/kg 13ac p.o. q.d. the survival curve was analyzed; (D) Ba/F-JAK2^{V617F}-bearing BALB/c-nude mice (*n* = 6) were treated for 20 consecutive days with 30 and 60 mg/kg 13ac p.o. q.d. On day 25, mice were sacrificed and spleen and liver weights determined. ***, *P* < 0.01 ANOVA, Dunnett's post test; (E) inhibition of the liver growth in the Ba/F-JAK2^{V617F} allograft model. ***, *P* < 0.01; **, 0.01 < *P* < 0.05 ANOVA, Dunnett's post test; and (F) spleen weight to body weight ratio in the Ba/F-JAK2^{V617F} allograft model.

CONCLUSIONS

Based on the progress made in JAK2/FLT3 dual target inhibitor **18e**, we designed selective 1,2,3,4-tetrahydro-isoquinolin series of JAK2 inhibitors. SAR developed around the designed cycle moieties combined with structure-based design led to the discovery of **13ac**, which possessed >14-fold selectivity over JAK1,3, FLT3 in enzyme assays. Full kinase spectrum screening indicated **13ac** possesses a relatively high selectivity. Furthermore, the western blot assay confirmed that the antitumor activities were indeed on-target. Compound **13ac** could also stimulate cell cycle arrest in the G₀/G₁ phase and induce tumor cell apoptosis. An efficacy study in a model of JAK2^{V617F}-driven disease demonstrated dose-dependent tumor growth inhibition and normalization of splenomegaly and hepatomegaly at well-

tolerated doses. To summarize, **13ac** is a promising inhibitor of JAK2 for the treatment of MPNs.

CHEMISTRY

The syntheses of the 4-(1*H*-pyrazol-4-yl)-pyrimidin-2-amine derivatives require the preparation of two pairs of building blocks, that is, 4-(1*H*-pyrazol-4-yl)-pyrimidine and anilines. The synthesis of amines is described in Scheme 1. The intermediate **2** was synthesized from commercially available phenethylamine by an amidation. Subsequently, the intermediate **2** was cyclized under concentrated sulfuric acid and paraformaldehyde to obtain intermediate **3**. Treatment of **3** with concentrated sulfuric acid and potassium nitrate at 0 °C provided **4a–b**, from which analogues without protection could be accessed. Compounds

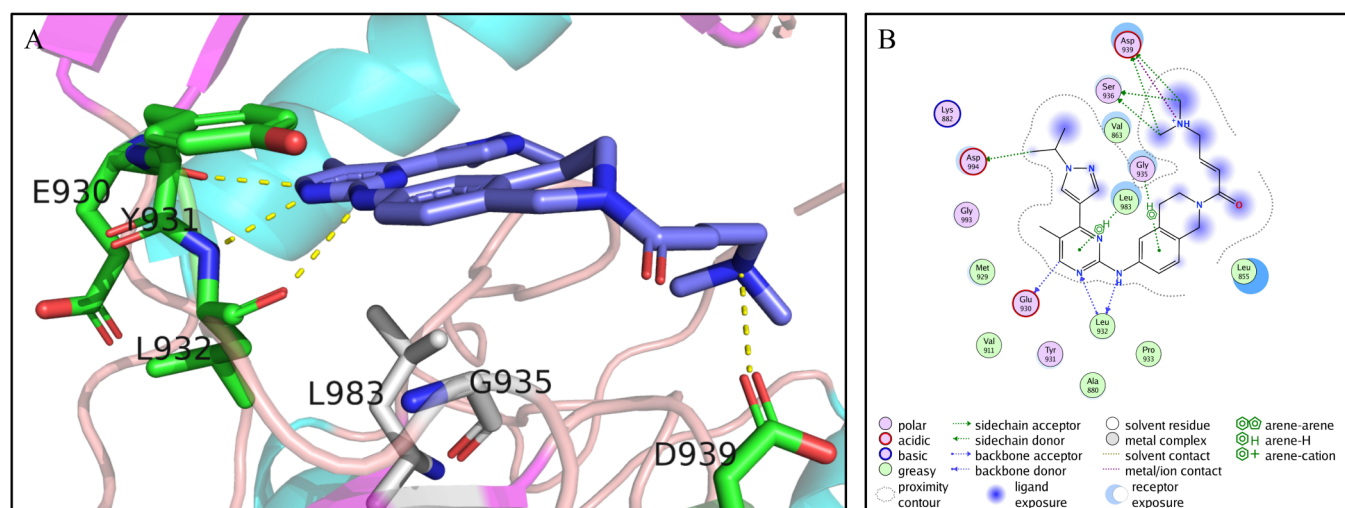


Figure 5. (A) 3D Model of **13ac** bound to the kinase catalytic domain of JAK2; **(B)** 2D Model of **13ac** bound to the kinase catalytic domain of JAK2 (PDB: 2XA4).

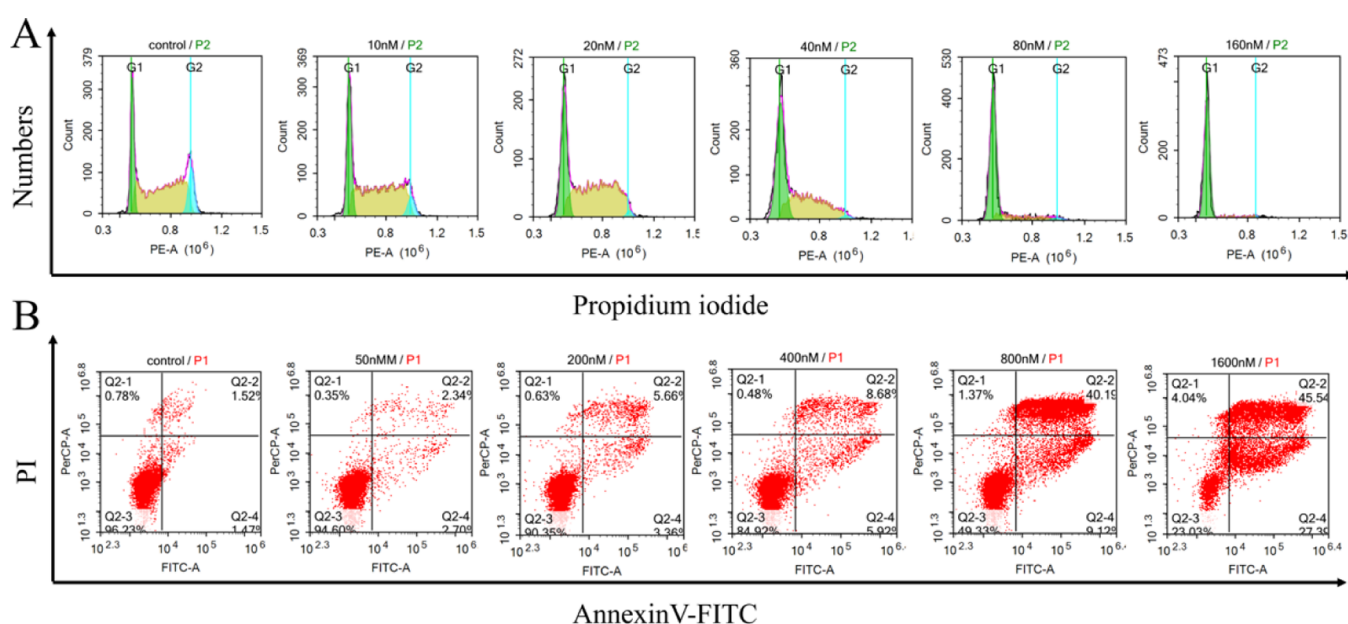


Figure 6. (A) Cell cycle effects of **13ac** on SET-2 cells. Cells were treated with increasing concentrations of **13ac** for 24 h, harvested, fixed, and stained with propidium iodide prior to flow cytometric analysis. **(B)** Effects of **13ac** on the induction of apoptosis. SET-2 cells were treated with **13ac** for 2 h at 0.05, 0.2, 0.4, 0.8, and 1.6 μM , respectively.

5a–b were further amidated under $(\text{BOC})_2\text{O}$. Primary amines (**7a–b**) were synthesized by hydrogen reduction.

The primary intermediates **10a–b** were synthesized via alkylation of **8** with 2-iodopropane to provide **9**, followed by the Suzuki reaction with 2, 4-dichloropyrimidine derivatives. The anilines (**7a–b**) and pyrimidine intermediates (**10a–b**) were coupled via a Buchwald–Hartwig reaction to get **11a–f**. The Boc groups were removed from **11a–f** with hydrochloric acid to produce the corresponding piperazines. The final products **13a–am** were obtained by alkylation or amidation (Scheme 2).

EXPERIMENTAL SECTION

Synthesis. All the chemical solvents and reagents were purchased from commercial sources and were used as received. Thin-layer chromatography was performed on 0.20 mm Silica Gel 60 F254 plates (Qingdao Haiyang Chemical, China) and visualized under UV light (254 nm). Flash column chromatography was carried out using fritted

solid loaders packed with Scharlau silica gel (0.04–0.06 mm) on Biotage FlashMaster Personal + flash chromatography. Counter-current Chromatography separations was finished with a SCU-Prep instrument manufactured by our team. The volume of the counter-current chromatography column is 1500 mL and the rotation speed is 1200 rpm. ^1H NMR and ^{13}C NMR spectra were recorded on a Bruker Avance 400 spectrometer (Bruker Company, Germany) or a Varian spectrometer (Varian, Palo Alto, CA), using TMS as an internal standard. Chemical shifts were given in ppm (parts per million). Mass spectra were recorded on a Q-TOF Premier mass spectrometer (Micromass, Manchester, UK). The purity of each compound (>95%) was determined on a Waters e2695 series LC system (column, Xtimate C18, 4.6 mm \times 150 mm, 5 μm ; mobile phase, methanol (60%)/ H_2O (40%); low rate, 1.0 mL/min; UV wavelength, 254–400 nm; temperature, 25 $^\circ\text{C}$; and injection volume, 10 μL).

2,2,2-Trifluoro-N-phenethylacetamide (2). To a solution of 2-phenylethan-1-amine (12.1 g, 0.1 mol) in acetonitrile (200 mL), K_2CO_3 (34.5 g, 0.25 mmol) and trifluoroacetic anhydride (17.0 mL, 0.12 mol) were added, and the mixture was stirred at room temperature

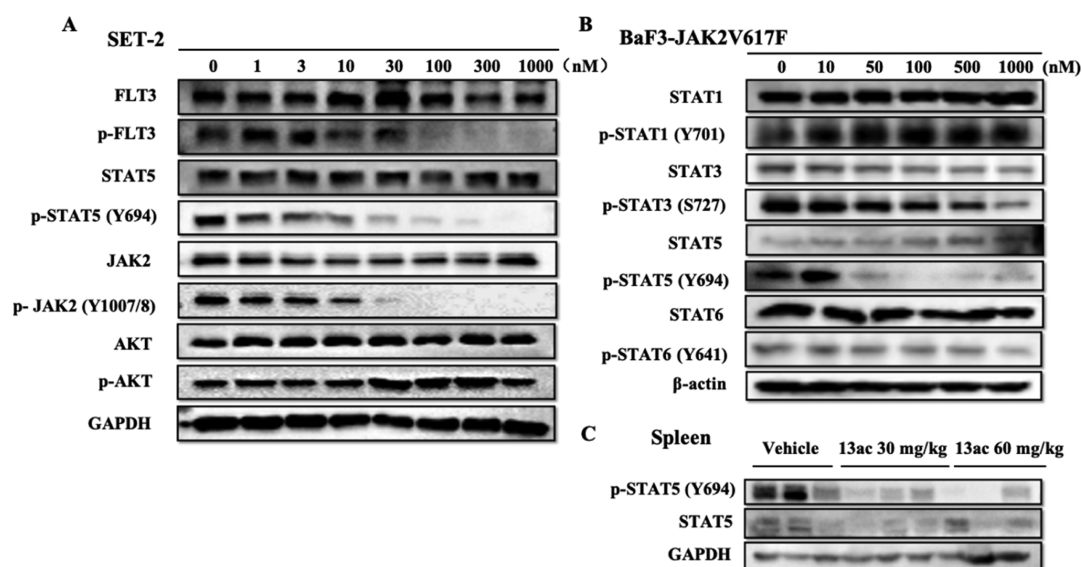
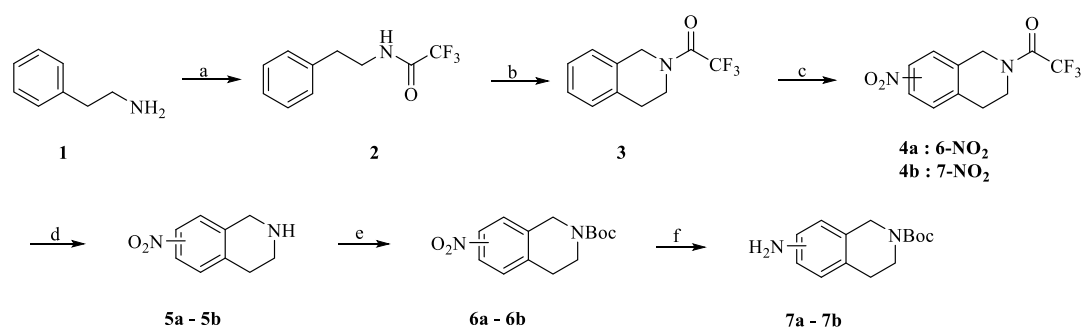


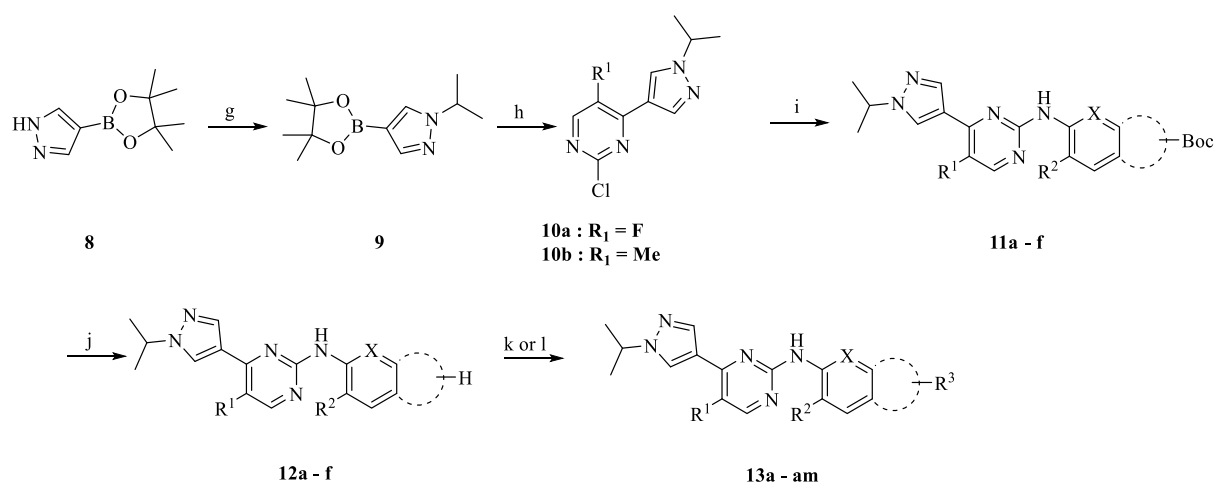
Figure 7. Inhibition of the JAK2 signaling pathway by 13ac. (A) SET-2, (B) Ba/F3 JAK2^{V617F} cells, and (C) spleen lysates of the Ba/F3 JAK2^{V617F} allograft model were treated for 3 h with 13ac. After lysis, the proteins were detected by immunoblotting with antibodies.

Scheme 1. Synthesis of Amino Derivatives 7a–b^a



^aReagents and conditions: (a) trifluoroacetic anhydride, K_2CO_3 , acetonitrile, rt; (b) paraformaldehyde, concentrated sulfuric acid, rt; (c) concentrated sulfuric acid, potassium nitrate, 0 °C; (d) hydrochloric acid, methanol, reflux; (e) (BOC)₂O, 60 °C; and (f) Pd/C, H₂, methanol, rt.

Scheme 2. Synthesis of 13a–am^a



^aReagents and conditions: (g) 2-iodopropane, K_2CO_3 , acetonitrile, reflux; (h) 2,4-dichloropyrimidine derivatives, dioxane/EtOH/water (v/v/v, 7/3/4), 80 °C, 2 h; (i) amines, dioxane, reflux, 4 h, N₂ atmosphere; (j) hydrochloric acid, EA, rt; (k) appropriate halide, K_2CO_3 , acetonitrile, rt. And (l) appropriate acid, HATU, DIEA, DCM, rt.

(rt) for 1 h. The completion of the reaction was checked with TLC on silica (silica gel: DCM/MeOH = 20:1). The mixture was dried under

reduced pressure. 50 mL of water was added to the concentrated solution, the solid was precipitated, filtered with suction, and dried to

obtain the title compound. Yield: 88%. ^1H NMR (400 MHz, Chloroform-*d*): δ 7.67 (t, *J* = 6.3 Hz, 1H), 7.33–7.24 (m, 2H), 7.25–7.16 (m, 3H), 3.46 (dt, *J* = 6.4, 5.6 Hz, 2H), 2.76 (tt, *J* = 5.6, 1.0 Hz, 2H). HRMS (ESI) *m/z*: 217.0774 [*M* + *H*⁺].

1-(3,4-Dihydroisoquinolin-2(1H)-yl)-2,2,2-trifluoroethan-1-one (3). To a solution of 2,2,2-trifluoro-*N*-phenethylacetamide (18.5 g, 0.085 mol) in concentrated sulfuric acid (100 mL) was slowly added paraformaldehyde (3.0 g, 0.1 mol), and the mixture was stirred at room temperature (rt) for 2 h. After the reaction completed, the mixture was very slowly added to ice water and extracted with ethyl acetate (200 mL) twice. The organic phases were collected together and concentrated under reduced pressure. The solid was washed with ether (50 mL) to obtain the title compound. Yield: 60%. ^1H NMR (400 MHz, Chloroform-*d*): δ 7.23 (ddt, *J* = 6.1, 3.9, 0.9 Hz, 1H), 7.20–7.11 (m, 3H), 4.55 (d, *J* = 1.0 Hz, 2H), 3.77 (dt, *J* = 8.6, 5.6 Hz, 2H), 2.90 (ddt, *J* = 8.7, 5.8, 0.7 Hz, 2H). HRMS (ESI) *m/z*: 229.0768 [*M* + *H*⁺].

2,2,2-Trifluoro-1-(6-nitro-3,4-dihydroisoquinolin-2(1H)-yl)ethan-1-one (4a). A solution of 1-(3,4-dihydroisoquinolin-2(1H)-yl)-2,2,2-trifluoroethan-1-one (11.0 g, 0.048 mol) in concentrated sulfuric acid (100 mL) was cooled to 0 °C, and potassium nitrate (12.1 g, 0.12 mol) was slowly added to the mixture while keeping the temperature below 0 °C. After 2 h, the reaction solution was very slowly added to ice water and extracted with ethyl acetate (150 mL) twice. The organic phases were collected together and concentrated under reduced pressure. The residue was pretreated by counter-current chromatography (solvent system: *n*-hexane/ethyl acetate/methanol/water 5:1:5:1; mobile phase: upper phase; rotation speed: 1200 rpm; and flow rate: 50 mL/min) and then purified by FlashMaster Personal + chromatography (silica gel: PE/EA = 90:10) to give the desired product **4a** and **4b**. ^1H NMR (400 MHz, Chloroform-*d*): δ 7.99 (dd, *J* = 8.2, 2.3 Hz, 1H), 7.78 (dt, *J* = 2.2, 1.0 Hz, 1H), 7.40 (dt, *J* = 8.2, 1.0 Hz, 1H), 4.59 (d, *J* = 1.0 Hz, 2H), 3.76 (ddd, *J* = 8.8, 6.0, 1.8 Hz, 2H), 2.94 (ddt, *J* = 8.4, 5.8, 1.1 Hz, 2H). HRMS (ESI) *m/z*: 274.0628 [*M* + *H*⁺].

6-Nitro-1,2,3,4-tetrahydroisoquinoline (5a). To a solution of 2,2,2-trifluoro-1-(6-nitro-3,4-dihydroisoquinolin-2(1H)-yl)ethan-1-one (7.8 g, 0.029 mol) in MeOH (60 mL) was added hydrochloric acid (10 mL) and refluxed for 2 h. The mixture was concentrated under reduced pressure and the desired product was obtained without purification. Yield: 94%. ^1H NMR (400 MHz, Chloroform-*d*): δ 7.96 (dd, *J* = 8.4, 2.2 Hz, 1H), 7.76 (dt, *J* = 2.1, 1.0 Hz, 1H), 7.32 (dt, *J* = 8.5, 1.0 Hz, 1H), 4.06 (dd, *J* = 7.5, 1.0 Hz, 2H), 3.00 (dddd, *J* = 7.8, 6.6, 5.9, 4.0 Hz, 2H), 2.86 (dddd, *J* = 11.6, 6.6, 3.8, 0.9 Hz, 2H), 2.66 (tt, *J* = 7.5, 5.9 Hz, 1H). HRMS (ESI) *m/z*: 179.0756 [*M* + *H*⁺].

tert-Butyl 6-Nitro-3,4-dihydroisoquinoline-2(1H)-carboxylate (6a). A solution of 6-nitro-1,2,3,4-tetrahydroisoquinoline (4.8 g, 0.027 mol) in (BOC)₂O (20 mL) was heated at 60 °C for 2 h, filtered, and washed with ether once to get the target compound. Yield: 90%. ^1H NMR (400 MHz, Chloroform-*d*): δ 7.99 (dd, *J* = 8.1, 2.3 Hz, 1H), 7.78 (dt, *J* = 2.1, 1.0 Hz, 1H), 7.28 (dt, *J* = 8.2, 1.0 Hz, 1H), 4.61 (d, *J* = 1.1 Hz, 2H), 3.73 (ddd, *J* = 9.1, 6.4, 4.2 Hz, 2H), 2.97 (ddd, *J* = 9.1, 6.4, 1.1 Hz, 2H), 1.47 (s, 7H). HRMS (ESI) *m/z*: 279.1356 [*M* + *H*⁺].

tert-Butyl 6-Amino-3,4-dihydroisoquinoline-2(1H)-carboxylate (7a). A solution of *tert*-butyl 6-nitro-3,4-dihydroisoquinoline-2(1H)-carboxylate (5.2 g, 0.024 mol) and Pd/C (0.52 g) in MeOH (50 mL) was reduced under the atmosphere of H₂. The mixture was filtered and concentrated to obtain the intermediate. Yield: 98%. ^1H NMR (400 MHz, Chloroform-*d*): δ 7.19 (dt, *J* = 8.3, 1.0 Hz, 1H), 6.60 (dd, *J* = 8.1, 2.3 Hz, 1H), 6.54 (dt, *J* = 2.1, 1.0 Hz, 1H), 4.75 (s, 1H), 4.59 (d, *J* = 0.9 Hz, 2H), 3.73 (dd, *J* = 9.1, 6.4 Hz, 2H), 2.82 (dddd, *J* = 9.2, 7.4, 6.4, 1.0 Hz, 2H), 1.47 (s, 6H). HRMS (ESI) *m/z*: 271.1567 [*M* + Na⁺].

The synthesis method of intermediates **9–12** was described in the previous literature, herein, we just described the synthesis of amide.

General Synthetic Procedure 1. Amidation. To a solution of secondary amine (0.01 mmol, 1.0 equiv), HATU (0.01 mmol, 1.0 equiv), and *N,N*-diisopropylethylamine (0.025 mmol, 2.5 equiv) in DCM (20 mL) was added acid (0.01 mmol, 1.0 equiv). The reaction mixture was stirred at room temperature for 0.5 h and filtered, and the solid was washed with EA to give the desired product.

3-(2-((4-(1-Isopropyl-1H-pyrazol-4-yl)-5-methylpyrimidin-2-yl)amino)-7,8-dihydro-1,6-naphthyridin-6(5H)-yl)propan-1-ol

(13a). ^1H NMR (400 MHz, DMSO-*d*₆): δ 9.19 (s, 1H), 8.38–8.30 (m, 2H), 8.11 (t, *J* = 4.2 Hz, 2H), 7.47 (d, *J* = 8.5 Hz, 1H), 4.63 (h, *J* = 6.6 Hz, 1H), 4.44 (d, *J* = 38.4 Hz, 1H), 3.55–3.44 (m, 4H), 2.80 (t, *J* = 5.9 Hz, 2H), 2.73 (t, *J* = 6.1 Hz, 2H), 2.54 (d, *J* = 7.1 Hz, 2H), 2.33 (s, 3H), 1.72–1.64 (m, 2H), 1.48 (d, *J* = 6.7 Hz, 6H). ^{13}C NMR (101 MHz, DMSO): δ 159.93, 158.01, 157.82, 152.89, 151.72, 139.55, 136.47, 129.69, 123.47, 120.45, 117.59, 110.21, 59.81, 55.19, 54.71, 53.83, 50.98, 32.20, 30.45, 23.03, 17.19. HRMS (ESI) *m/z*: 408.5245 [*M* + *H*⁺].

2-(5-((4-(1-Isopropyl-1H-pyrazol-4-yl)-5-methylpyrimidin-2-yl)amino)indolin-1-yl)ethan-1-ol (13b). ^1H NMR (400 MHz, DMSO-*d*₆): δ 8.90 (s, 1H), 8.24 (d, *J* = 41.8 Hz, 2H), 8.05 (s, 1H), 7.49 (s, 1H), 7.34 (d, *J* = 8.4 Hz, 1H), 6.45 (d, *J* = 8.4 Hz, 1H), 4.63 (dq, *J* = 20.3, 6.8, 6.1 Hz, 2H), 3.61 (q, *J* = 6.1 Hz, 2H), 3.31 (d, *J* = 8.9 Hz, 1H), 3.05 (t, *J* = 6.3 Hz, 2H), 2.87 (t, *J* = 8.2 Hz, 2H), 2.28 (s, 3H), 1.47 (d, *J* = 6.7 Hz, 6H). ^{13}C NMR (101 MHz, DMSO): δ 159.79, 159.38, 157.61, 148.07, 139.29, 132.27, 129.86, 129.27, 120.84, 118.60, 117.13, 115.43, 107.01, 59.57, 54.30, 53.78, 52.86, 29.01, 23.04, 17.11. HRMS (ESI) *m/z*: 379.4856 [*M* + *H*⁺].

2-(5-((4-(1-Isopropyl-1H-pyrazol-4-yl)-5-methylpyrimidin-2-yl)amino)isoindolin-2-yl)ethan-1-ol (13c). ^1H NMR (400 MHz, DMSO-*d*₆): δ 9.29 (s, 1H), 8.30 (d, *J* = 21.5 Hz, 2H), 8.08 (s, 1H), 7.76 (s, 1H), 7.54 (d, *J* = 8.2 Hz, 1H), 7.12 (d, *J* = 8.2 Hz, 1H), 4.63 (p, *J* = 6.7 Hz, 1H), 4.51 (s, 1H), 3.85 (d, *J* = 20.6 Hz, 4H), 3.64–3.47 (m, 2H), 2.76 (t, *J* = 6.3 Hz, 2H), 2.31 (s, 3H), 1.48 (d, *J* = 6.7 Hz, 6H). ^{13}C NMR (101 MHz, DMSO): δ 159.84, 159.00, 157.71, 140.81, 140.30, 139.34, 132.79, 129.43, 122.29, 120.66, 117.42, 116.47, 112.67, 60.46, 59.70, 59.04, 58.44, 53.82, 23.03, 17.15. HRMS (ESI) *m/z*: 379.4866 [*M* + *H*⁺].

2-(6-((4-(1-Isopropyl-1H-pyrazol-4-yl)-5-methylpyrimidin-2-yl)amino)-3,4-dihydroisoquinolin-2(1H)-yl)ethan-1-ol (13d). ^1H NMR (400 MHz, DMSO-*d*₆): δ 9.20 (s, 1H), 8.29 (d, *J* = 22.7 Hz, 2H), 8.08 (s, 1H), 7.65 (d, *J* = 2.3 Hz, 1H), 7.46 (dd, *J* = 8.3, 2.3 Hz, 1H), 6.94 (d, *J* = 8.4 Hz, 1H), 4.62 (h, *J* = 6.6 Hz, 1H), 4.46 (s, 1H), 3.67–3.46 (m, 4H), 2.80 (d, *J* = 5.8 Hz, 2H), 2.71 (t, *J* = 5.8 Hz, 2H), 2.57 (t, *J* = 6.2 Hz, 2H), 2.31 (s, 3H), 1.48 (d, *J* = 6.7 Hz, 6H). ^{13}C NMR (101 MHz, DMSO): δ 159.88, 159.00, 157.63, 139.42, 139.31, 134.44, 129.38, 127.92, 126.71, 120.74, 118.31, 116.72, 116.35, 60.74, 59.30, 56.07, 53.83, 51.64, 29.63, 23.03, 17.15. HRMS (ESI) *m/z*: 393.5070 [*M* + *H*⁺].

3-(6-((4-(1-Isopropyl-1H-pyrazol-4-yl)-5-methylpyrimidin-2-yl)amino)-3,4-dihydroisoquinolin-2(1H)-yl)propan-1-ol (13e). ^1H NMR (400 MHz, DMSO-*d*₆): δ 9.20 (s, 1H), 8.32 (s, 1H), 8.26 (s, 1H), 8.08 (s, 1H), 7.65 (d, *J* = 2.2 Hz, 1H), 7.47 (dd, *J* = 8.3, 2.3 Hz, 1H), 6.95 (d, *J* = 8.3 Hz, 1H), 4.75–4.39 (m, 2H), 3.57–3.42 (m, 4H), 2.80 (t, *J* = 5.8 Hz, 2H), 2.64 (t, *J* = 5.9 Hz, 2H), 2.50 (s, 2H), 2.31 (s, 3H), 1.68 (p, *J* = 6.5 Hz, 2H), 1.48 (d, *J* = 6.7 Hz, 6H). ^{13}C NMR (101 MHz, DMSO): δ 159.89, 159.00, 157.64, 139.46, 139.31, 134.46, 129.39, 127.83, 126.75, 120.74, 118.30, 116.75, 116.36, 59.96, 55.86, 55.56, 53.83, 51.25, 30.34, 29.66, 23.04, 17.15. HRMS (ESI) *m/z*: 407.5340 [*M* + *H*⁺].

1-(6-((5-Fluoro-4-(1-isopropyl-1H-pyrazol-4-yl)pyrimidin-2-yl)amino)-3,4-dihydroisoquinolin-2(1H)-yl)-2-hydroxyethan-1-one (13f). ^1H NMR (400 MHz, DMSO-*d*₆): δ 9.55 (d, *J* = 4.7 Hz, 1H), 8.44 (d, *J* = 45.8 Hz, 2H), 8.09 (s, 1H), 7.68 (s, 1H), 7.55 (t, *J* = 6.6 Hz, 1H), 7.11 (dd, *J* = 13.3, 8.1 Hz, 1H), 4.76–4.42 (m, 4H), 4.19 (d, *J* = 5.2 Hz, 2H), 3.64 (dt, *J* = 51.4, 5.8 Hz, 2H), 2.83 (dt, *J* = 28.2, 5.8 Hz, 2H), 1.48 (d, *J* = 6.6 Hz, 6H). ^{13}C NMR (101 MHz, DMSO): δ 170.87, 156.92, 150.02, 147.54, 146.90, 146.25, 139.54, 138.88, 134.92, 129.87, 126.97, 126.44, 118.39, 117.31, 115.71, 60.74, 54.01, 43.89, 41.70, 29.42, 22.96. HRMS (ESI) *m/z*: 411.4546 [*M* + *H*⁺].

***N*-(3-Chlorophenyl)-6-((4-(1-isopropyl-1H-pyrazol-4-yl)-5-methylpyrimidin-2-yl)amino)-3,4-dihydroisoquinoline-2(1H)-carboxamide (13g).** ^1H NMR (400 MHz, DMSO-*d*₆): δ 9.30 (s, 1H), 8.73 (s, 1H), 8.31 (d, *J* = 21.9 Hz, 2H), 8.09 (s, 1H), 7.72 (d, *J* = 26.0 Hz, 2H), 7.57 (d, *J* = 8.3 Hz, 1H), 7.45 (d, *J* = 8.3 Hz, 1H), 7.26 (t, *J* = 8.1 Hz, 1H), 7.09 (d, *J* = 8.4 Hz, 1H), 6.98 (d, *J* = 7.9 Hz, 1H), 4.61 (d, *J* = 16.3 Hz, 3H), 3.71 (t, *J* = 5.8 Hz, 2H), 2.85 (t, *J* = 5.9 Hz, 2H), 2.32 (s, 3H), 1.49 (d, *J* = 6.7 Hz, 6H). ^{13}C NMR (101 MHz, DMSO): δ 159.90, 158.95, 157.69, 155.14, 142.73, 139.93, 139.34, 135.07, 133.20, 130.35,

129.44, 126.68, 126.38, 121.69, 120.70, 119.38, 118.38, 118.27, 117.16, 116.57, 53.84, 45.80, 41.95, 29.27, 23.04, 17.16. HRMS (ESI) m/z : 503.0190 $[M + H]^+$.

N-Ethyl-6-((4-(1-isopropyl-1H-pyrazol-4-yl)-5-methylpyrimidin-2-yl)amino)-3,4-dihydroisoquinoline-2(1H)-carboxamide (13h). ^1H NMR (400 MHz, DMSO- d_6): δ 9.26 (s, 1H), 8.30 (d, J = 22.7 Hz, 2H), 8.08 (s, 1H), 7.70 (d, J = 2.2 Hz, 1H), 7.53 (dd, J = 8.3, 2.3 Hz, 1H), 7.03 (d, J = 8.3 Hz, 1H), 6.49 (t, J = 5.4 Hz, 1H), 4.62 (h, J = 6.5 Hz, 1H), 4.41 (s, 2H), 3.54 (t, J = 5.8 Hz, 2H), 3.08 (dt, J = 12.5, 6.3 Hz, 2H), 2.75 (t, J = 5.9 Hz, 2H), 2.31 (s, 3H), 1.48 (d, J = 6.6 Hz, 6H), 1.03 (t, J = 7.1 Hz, 3H). ^{13}C NMR (101 MHz, DMSO): δ 159.90, 158.95, 157.80, 157.67, 139.71, 139.32, 135.21, 129.43, 126.95, 126.59, 120.70, 118.43, 117.08, 116.51, 53.83, 45.46, 41.38, 35.38, 29.23, 23.04, 17.15, 16.15. HRMS (ESI) m/z : 320.5330 $[M + H]^+$.

3-(6-((5-Fluoro-4-(1-isopropyl-1H-pyrazol-4-yl)pyrimidin-2-yl)amino)-3,4-dihydroisoquinolin-2(1H)-yl)propan-1-ol (13i). ^1H NMR (400 MHz, DMSO- d_6): δ 10.24 (s, 1H), 9.68 (s, 1H), 8.53 (d, J = 3.0 Hz, 1H), 8.40 (d, J = 2.0 Hz, 1H), 8.10 (d, J = 1.1 Hz, 1H), 7.76 (d, J = 2.2 Hz, 1H), 7.60 (dd, J = 8.4, 2.2 Hz, 1H), 7.14 (d, J = 8.5 Hz, 1H), 4.67 (p, J = 6.6 Hz, 1H), 4.25 (d, J = 36.4 Hz, 2H), 3.37 (s, 4H), 3.24 (t, J = 8.1 Hz, 2H), 3.12 (s, 2H), 1.94 (dq, J = 11.9, 6.0 Hz, 2H), 1.48 (d, J = 6.6 Hz, 6H). ^{13}C NMR (101 MHz, DMSO): δ 156.98, 149.96, 147.48, 146.97, 146.18, 139.09, 138.86, 134.51, 128.24, 126.82, 118.38, 116.85, 115.73, 59.94, 55.80, 55.52, 54.00, 51.18, 30.28, 29.56, 22.94. HRMS (ESI) m/z : 411.4974 $[M + H]^+$.

6-((4-(1-isopropyl-1H-pyrazol-4-yl)-5-methylpyrimidin-2-yl)amino)-N-propyl-3,4-dihydroisoquinoline-2(1H)-carboxamide (13j). ^1H NMR (400 MHz, DMSO- d_6): δ 9.26 (s, 1H), 8.30 (d, J = 22.9 Hz, 2H), 8.09 (s, 1H), 7.71 (d, J = 2.2 Hz, 1H), 7.54 (dd, J = 8.4, 2.2 Hz, 1H), 7.03 (d, J = 8.3 Hz, 1H), 6.50 (t, J = 5.5 Hz, 1H), 4.63 (hept, J = 6.7 Hz, 1H), 4.43 (s, 2H), 3.55 (t, J = 5.8 Hz, 2H), 3.02 (q, J = 7.8, 7.0 Hz, 2H), 2.76 (t, J = 5.8 Hz, 2H), 2.32 (s, 3H), 1.46 (dd, J = 18.8, 6.9 Hz, 8H), 0.84 (t, J = 7.4 Hz, 3H). ^{13}C NMR (101 MHz, DMSO): δ 159.90, 158.95, 157.88, 157.67, 139.70, 139.32, 135.21, 129.43, 126.99, 126.60, 120.70, 118.43, 117.08, 116.51, 53.83, 45.50, 42.47, 41.44, 29.22, 23.56, 23.04, 17.15, 11.87. HRMS (ESI) m/z : 434.5600 $[M + H]^+$.

2-(7-Fluoro-6-((4-(1-isopropyl-1H-pyrazol-4-yl)-5-methylpyrimidin-2-yl)amino)-3,4-dihydroisoquinolin-2(1H)-yl)ethan-1-ol (13k). ^1H NMR (400 MHz, DMSO- d_6): δ 8.56 (s, 1H), 8.26 (d, J = 25.6 Hz, 2H), 8.01 (s, 1H), 7.67 (d, J = 8.0 Hz, 1H), 6.92 (d, J = 11.5 Hz, 1H), 4.61 (p, J = 6.7 Hz, 1H), 4.54 (s, 1H), 3.82–3.42 (m, 4H), 2.96–2.63 (m, 4H), 2.55 (t, J = 6.5 Hz, 2H), 2.30 (s, 3H), 1.46 (d, J = 6.6 Hz, 6H). ^{13}C NMR (101 MHz, DMSO): δ 159.91, 159.09, 157.81, 154.07, 151.66, 139.34, 130.75, 129.94, 129.42, 123.69, 120.56, 116.87, 113.15, 60.46, 59.27, 55.69, 53.82, 51.37, 28.78, 23.02, 17.08. HRMS (ESI) m/z : 411.4974 $[M + H]^+$.

2-(6-((5-Fluoro-4-(1-isopropyl-1H-pyrazol-4-yl)pyrimidin-2-yl)amino)-3,4-dihydroisoquinolin-2(1H)-yl)ethan-1-ol (13l). ^1H NMR (400 MHz, DMSO- d_6): δ 9.49 (s, 1H), 8.49 (d, J = 2.9 Hz, 1H), 8.38 (s, 1H), 8.08 (s, 1H), 7.62 (s, 1H), 7.48 (d, J = 8.3 Hz, 1H), 6.99 (d, J = 8.4 Hz, 1H), 4.66 (td, J = 14.4, 13.9, 7.2 Hz, 2H), 3.83–3.50 (m, 4H), 2.78 (d, J = 66.0 Hz, 6H), 1.48 (d, J = 6.7 Hz, 6H). ^{13}C NMR (101 MHz, DMSO): δ 53.94, 147.50, 143.35, 142.60, 139.98, 138.80, 132.96, 128.37, 127.01, 126.49, 120.09, 118.70, 117.83, 59.30, 56.76, 56.40, 54.17, 51.12, 28.89, 23.16. HRMS (ESI) m/z : 397.4704 $[M + H]^+$.

4-(6-((5-Fluoro-4-(1-isopropyl-1H-pyrazol-4-yl)pyrimidin-2-yl)amino)-3,4-dihydroisoquinolin-2(1H)-yl)butan-1-ol (13m). ^1H NMR (400 MHz, DMSO- d_6): δ 9.48 (s, 1H), 8.49 (d, J = 3.0 Hz, 1H), 8.38 (d, J = 1.9 Hz, 1H), 8.08 (d, J = 1.3 Hz, 1H), 7.60 (d, J = 2.2 Hz, 1H), 7.46 (dd, J = 8.3, 2.2 Hz, 1H), 6.98 (d, J = 8.4 Hz, 1H), 4.68 (h, J = 6.6 Hz, 1H), 4.56 (s, 1H), 3.42 (t, J = 6.3 Hz, 2H), 2.81 (t, J = 5.9 Hz, 2H), 2.64 (t, J = 5.8 Hz, 2H), 2.44 (t, J = 7.1 Hz, 2H), 1.60–1.40 (m, 10H). ^{13}C NMR (101 MHz, DMSO): δ 157.01, 149.95, 147.47, 146.97, 145.96, 139.05, 138.85, 134.58, 129.78, 128.38, 126.82, 118.39, 116.83, 115.73, 61.22, 58.22, 55.74, 54.00, 51.11, 31.13, 29.61, 23.80, 22.95. HRMS (ESI) m/z : 424.5244 $[M + H]^+$.

5-(6-((5-Fluoro-4-(1-isopropyl-1H-pyrazol-4-yl)pyrimidin-2-yl)amino)-3,4-dihydroisoquinolin-2(1H)-yl)pentan-1-ol (13n). ^1H NMR (400 MHz, DMSO- d_6): δ 9.46 (s, 1H), 8.49 (d, J = 3.0 Hz, 1H), 8.38 (d, J = 1.6 Hz, 1H), 8.08 (s, 1H), 7.59 (s, 1H), 7.46 (dd, J =

8.4, 1.9 Hz, 2H), 6.98 (d, J = 8.3 Hz, 1H), 4.67 (dt, J = 13.3, 6.6 Hz, 2H), 4.35 (t, J = 4.9 Hz, 2H), 3.50 (s, 1H), 3.44–3.37 (m, 5H), 2.86–2.75 (m, 4H), 2.66 (s, 0H), 2.44 (d, J = 5.0 Hz, 1H), 1.58–1.40 (m, 8H), 1.33 (dt, J = 15.3, 7.1 Hz, 3H). HRMS (ESI) m/z : 439.5514 $[M + H]^+$.

4-(6-((4-(1-isopropyl-1H-pyrazol-4-yl)-5-methylpyrimidin-2-yl)amino)-3,4-dihydroisoquinolin-2(1H)-yl)butan-1-ol (13o). ^1H NMR (400 MHz, DMSO- d_6): δ 9.19 (s, 1H), 8.29 (d, J = 23.0 Hz, 2H), 8.08 (s, 1H), 7.64 (d, J = 2.3 Hz, 1H), 7.46 (dd, J = 8.3, 2.3 Hz, 1H), 6.95 (d, J = 8.4 Hz, 1H), 4.63 (q, J = 6.6 Hz, 1H), 4.56 (d, J = 26.0 Hz, 1H), 3.56–3.35 (m, 4H), 2.80 (t, J = 5.9 Hz, 2H), 2.63 (t, J = 5.8 Hz, 2H), 2.43 (t, J = 7.0 Hz, 2H), 2.31 (s, 3H), 1.55 (q, J = 7.2 Hz, 2H), 1.48 (d, J = 6.7 Hz, 6H). ^{13}C NMR (101 MHz, DMSO): δ 159.03, 158.27, 158.19, 140.86, 139.50, 131.80, 129.78, 127.32, 121.05, 120.48, 118.02, 117.76, 116.99, 60.49, 60.22, 55.58, 53.89, 52.27, 49.47, 29.86, 29.68, 25.74, 23.02, 22.91, 21.01, 17.16. HRMS (ESI) m/z : 421.5610 $[M + H]^+$.

5-(6-((4-(1-isopropyl-1H-pyrazol-4-yl)-5-methylpyrimidin-2-yl)amino)-3,4-dihydroisoquinolin-2(1H)-yl)pentan-1-ol (13p). ^1H NMR (400 MHz, DMSO- d_6): δ 9.19 (s, 1H), 8.32 (s, 1H), 8.27 (s, 1H), 8.08 (s, 1H), 7.65 (d, J = 2.2 Hz, 1H), 7.47 (dd, J = 8.3, 2.3 Hz, 1H), 6.95 (d, J = 8.3 Hz, 1H), 4.63 (p, J = 6.7 Hz, 1H), 4.34 (s, 1H), 3.40 (t, J = 5.7 Hz, 2H), 2.80 (t, J = 5.9 Hz, 2H), 2.63 (t, J = 5.9 Hz, 2H), 2.43 (t, J = 7.3 Hz, 2H), 2.31 (s, 3H), 1.58–1.41 (m, 10H), 1.35 (qd, J = 9.8, 8.4, 4.5 Hz, 2H). ^{13}C NMR (101 MHz, DMSO): δ 158.46, 157.32, 157.25, 152.31, 138.89, 133.23, 128.99, 125.84, 125.17, 122.18, 119.75, 119.28, 117.87, 62.50, 55.23, 54.16, 51.07, 31.69, 28.71, 27.04, 24.94, 23.19, 15.49. HRMS (ESI) m/z : 435.5880 $[M + H]^+$.

2-(2-Ethoxyethyl)-N-(4-(1-isopropyl-1H-pyrazol-4-yl)-5-methylpyrimidin-2-yl)-1,2,3,4-tetrahydroisoquinolin-6-amine (13q). ^1H NMR (400 MHz, DMSO- d_6): δ 9.20 (s, 1H), 8.30 (d, J = 22.7 Hz, 2H), 8.08 (s, 1H), 7.65 (d, J = 2.2 Hz, 1H), 7.47 (dd, J = 8.3, 2.2 Hz, 1H), 6.94 (d, J = 8.3 Hz, 1H), 4.63 (hept, J = 6.7 Hz, 1H), 3.61–3.51 (m, 4H), 3.46 (q, J = 7.0 Hz, 2H), 2.79 (d, J = 5.8 Hz, 2H), 2.70 (t, J = 5.8 Hz, 2H), 2.64 (t, J = 6.0 Hz, 2H), 2.31 (s, 3H), 1.49 (d, J = 6.7 Hz, 6H), 1.12 (t, J = 7.0 Hz, 3H). ^{13}C NMR (101 MHz, DMSO): δ 159.87, 159.01, 157.63, 139.46, 139.32, 134.35, 129.35, 127.83, 126.68, 120.76, 118.31, 116.74, 116.34, 68.48, 65.94, 57.73, 56.03, 53.83, 51.59, 29.65, 23.02, 17.15, 15.62. HRMS (ESI) m/z : 421.5610 $[M + H]^+$.

2-Butyl-N-(4-(1-isopropyl-1H-pyrazol-4-yl)-5-methylpyrimidin-2-yl)-1,2,3,4-tetrahydroisoquinolin-6-amine (13r). ^1H NMR (400 MHz, DMSO- d_6): δ 9.19 (s, 1H), 8.29 (d, J = 23.5 Hz, 2H), 8.09 (s, 1H), 7.65 (s, 1H), 7.47 (d, J = 7.7 Hz, 1H), 6.94 (d, J = 8.2 Hz, 1H), 4.70–4.56 (m, J = 6.8 Hz, 1H), 3.46 (s, 2H), 2.79 (s, 2H), 2.61 (s, 2H), 2.41 (s, 2H), 2.31 (s, 3H), 1.48 (d, J = 6.8 Hz, 8H), 1.31 (p, J = 7.3 Hz, 2H), 0.90 (t, J = 7.2 Hz, 3H). ^{13}C NMR (101 MHz, DMSO- d_6): δ 159.88, 158.98, 157.65, 139.71, 139.32, 134.06, 129.40, 126.80, 120.72, 118.22, 116.86, 116.43, 57.61, 55.28, 53.83, 50.97, 29.10, 28.73, 23.03, 20.51, 17.16, 14.34. HRMS (ESI) m/z : 405.5620 $[M + H]^+$.

2-Allyl-N-(4-(1-isopropyl-1H-pyrazol-4-yl)-5-methylpyrimidin-2-yl)-1,2,3,4-tetrahydroisoquinolin-6-amine (13s). ^1H NMR (400 MHz, DMSO- d_6): δ 9.21 (s, 1H), 8.33 (s, 1H), 8.27 (d, J = 0.8 Hz, 1H), 8.08 (s, 1H), 7.66 (d, J = 2.2 Hz, 1H), 7.47 (dd, J = 8.3, 2.2 Hz, 1H), 6.95 (d, J = 8.3 Hz, 1H), 5.91 (ddt, J = 16.6, 10.2, 6.3 Hz, 1H), 5.26 (dq, J = 17.2, 1.7 Hz, 1H), 5.18 (ddt, J = 10.1, 2.2, 1.2 Hz, 1H), 4.62 (h, J = 6.7 Hz, 1H), 3.48 (s, 2H), 3.12 (dt, J = 6.4, 1.4 Hz, 2H), 2.81 (t, J = 5.9 Hz, 2H), 2.65 (t, J = 5.8 Hz, 2H), 2.31 (s, 3H), 1.49 (d, J = 6.6 Hz, 6H). ^{13}C NMR (101 MHz, DMSO): δ 159.87, 159.01, 157.64, 139.49, 139.32, 136.22, 134.40, 129.36, 127.75, 126.70, 120.75, 118.35, 117.80, 116.77, 116.35, 61.23, 55.59, 53.83, 50.75, 29.62, 23.03, 17.16. HRMS (ESI) m/z : 389.5190 $[M + H]^+$.

2-(6-((4-(1-isopropyl-1H-pyrazol-4-yl)-5-methylpyrimidin-2-yl)amino)-3,4-dihydroisoquinolin-2(1H)-yl)acetone nitrile (13t). ^1H NMR (400 MHz, DMSO- d_6): δ 9.24 (s, 1H), 8.30 (d, J = 21.8 Hz, 2H), 8.09 (s, 1H), 7.69 (d, J = 2.3 Hz, 1H), 7.51 (dd, J = 8.3, 2.2 Hz, 1H), 7.00 (d, J = 8.4 Hz, 1H), 4.63 (hept, J = 6.7 Hz, 1H), 3.91 (s, 2H), 3.62 (s, 2H), 2.86 (d, J = 6.0 Hz, 2H), 2.77 (d, J = 5.7 Hz, 2H), 2.32 (s, 3H), 1.49 (d, J = 6.7 Hz, 6H). ^{13}C NMR (101 MHz, DMSO): δ 159.87, 158.97, 157.66, 139.77, 139.34, 133.54, 129.35, 126.77, 126.45, 120.74, 118.35, 116.96, 116.47, 116.34, 53.85, 53.79, 49.74, 45.59, 29.43, 23.01, 17.16. HRMS (ESI) m/z : 388.4910 $[M + H]^+$.

3-(6-((4-(1-isopropyl-1H-pyrazol-4-yl)-5-methylpyrimidin-2-yl)amino)-3,4-dihydroisoquinolin-2(1H)-yl)propanenitrile (13u). ¹H NMR (400 MHz, DMSO-*d*₆): δ 9.21 (s, 1H), 8.29 (d, *J* = 22.7 Hz, 2H), 8.08 (s, 1H), 7.67 (d, *J* = 2.2 Hz, 1H), 7.48 (dd, *J* = 8.3, 2.2 Hz, 1H), 6.95 (d, *J* = 8.3 Hz, 1H), 4.63 (hept, *J* = 6.7 Hz, 1H), 2.76 (ddt, *J* = 20.6, 9.8, 5.7 Hz, 8H), 2.31 (s, 3H), 1.48 (d, *J* = 6.6 Hz, 6H). ¹³C NMR (101 MHz, DMSO-*d*₆): δ 159.89, 158.98, 157.64, 139.57, 139.31, 134.24, 129.40, 127.33, 126.74, 120.73, 120.50, 118.32, 116.81, 116.41, 54.95, 53.83, 53.09, 50.51, 29.46, 23.03, 17.15, 15.80. HRMS (ESI) *m/z*: 402.5180 [M + H⁺].

N-(4-(1-isopropyl-1H-pyrazol-4-yl)-5-methylpyrimidin-2-yl)-2-(prop-2-yn-1-yl)-1,2,3,4-tetrahydroisoquinolin-6-amine (13v). ¹H NMR (400 MHz, DMSO-*d*₆): δ 9.22 (s, 1H), 8.30 (d, *J* = 22.4 Hz, 2H), 8.09 (s, 1H), 7.75–7.61 (m, 1H), 7.56–7.42 (m, 1H), 6.98 (d, *J* = 8.4 Hz, 1H), 4.63 (p, *J* = 6.7 Hz, 1H), 3.59 (s, 2H), 3.51–3.40 (m, 2H), 3.23–3.13 (m, 1H), 2.84 (s, 2H), 2.72 (s, 2H), 2.32 (s, 3H), 1.49 (d, *J* = 6.7 Hz, 6H). ¹³C NMR (101 MHz, DMSO): δ 159.89, 158.99, 157.65, 139.51, 139.32, 133.99, 129.39, 127.46, 126.76, 120.73, 118.34, 116.82, 116.40, 79.84, 76.20, 53.90, 53.83, 49.71, 46.51, 29.64, 23.04, 17.15. HRMS (ESI) *m/z*: 387.5030 [M + H⁺].

2-(But-2-yn-1-yl)-N-(4-(1-isopropyl-1H-pyrazol-4-yl)-5-methylpyrimidin-2-yl)-1,2,3,4-tetrahydroisoquinolin-6-amine (13w). ¹H NMR (400 MHz, DMSO-*d*₆): δ 9.21 (s, 1H), 8.33 (s, 1H), 8.27 (s, 1H), 8.08 (s, 1H), 7.66 (d, *J* = 2.3 Hz, 1H), 7.48 (dd, *J* = 8.4, 2.2 Hz, 1H), 6.97 (d, *J* = 8.4 Hz, 1H), 4.63 (hept, *J* = 6.7 Hz, 1H), 3.38 (q, *J* = 2.4 Hz, 2H), 2.82 (t, *J* = 5.8 Hz, 2H), 2.70 (t, *J* = 5.9 Hz, 2H), 2.32 (s, 3H), 1.83 (t, *J* = 2.3 Hz, 3H), 1.49 (d, *J* = 6.6 Hz, 6H). ¹³C NMR (101 MHz, DMSO): δ 159.88, 159.00, 157.65, 139.47, 139.32, 134.07, 129.38, 127.60, 126.75, 120.74, 118.31, 116.78, 116.38, 81.12, 75.17, 54.12, 53.83, 49.85, 47.01, 29.68, 23.03, 17.15, 3.55. HRMS (ESI) *m/z*: 401.5300 [M + H⁺].

Methyl-(E)-4-(6-((4-(1-isopropyl-1H-pyrazol-4-yl)-5-methylpyrimidin-2-yl)amino)-3,4-dihydroisoquinolin-2(1H)-yl)but-2-enoate (13x). ¹H NMR (400 MHz, DMSO-*d*₆): δ 9.22 (s, 1H), 8.33 (s, 1H), 8.29 (s, 1H), 8.08 (s, 1H), 7.67 (d, *J* = 2.2 Hz, 1H), 7.52–7.44 (m, 1H), 6.96 (d, *J* = 8.8 Hz, 2H), 6.10 (d, *J* = 15.7 Hz, 1H), 4.63 (hept, *J* = 6.7 Hz, 1H), 3.68 (s, 3H), 3.52 (s, 2H), 2.83 (t, *J* = 5.8 Hz, 2H), 2.68 (t, *J* = 5.8 Hz, 2H), 2.32 (s, 3H), 1.49 (d, *J* = 6.6 Hz, 6H). ¹³C NMR (101 MHz, DMSO): δ 166.38, 159.88, 158.99, 157.64, 146.64, 139.58, 139.31, 134.22, 129.37, 127.43, 126.73, 122.53, 120.74, 118.34, 116.78, 116.39, 58.56, 55.68, 53.83, 51.80, 50.99, 29.53, 23.02, 17.15. HRMS (ESI) *m/z*: 447.5550 [M + H⁺].

Methyl-4-(6-((4-(1-isopropyl-1H-pyrazol-4-yl)-5-methylpyrimidin-2-yl)amino)-3,4-dihydroisoquinolin-2(1H)-yl)butanoate (13y). ¹H NMR (400 MHz, DMSO-*d*₆): δ 9.18 (s, 1H), 8.32 (s, 1H), 8.26 (s, 1H), 8.07 (s, 1H), 7.64 (s, 1H), 7.46 (d, *J* = 8.4 Hz, 1H), 6.95 (d, *J* = 8.3 Hz, 1H), 4.62 (dt, *J* = 13.2, 6.6 Hz, 1H), 3.57 (d, *J* = 9.1 Hz, 3H), 3.46 (s, 2H), 2.78 (d, *J* = 5.3 Hz, 2H), 2.62 (t, *J* = 5.6 Hz, 2H), 2.44 (t, *J* = 6.9 Hz, 2H), 2.36 (t, *J* = 7.2 Hz, 2H), 2.31 (s, 3H), 1.83–1.74 (m, 2H), 1.48 (d, *J* = 6.6 Hz, 6H). ¹³C NMR (101 MHz, DMSO): δ 173.86, 159.90, 158.99, 157.63, 139.44, 139.31, 134.48, 129.40, 127.83, 126.74, 120.73, 118.28, 116.72, 116.36, 57.30, 55.71, 53.83, 51.61, 51.04, 31.80, 29.63, 23.04, 22.51, 17.14. HRMS (ESI) *m/z*: 449.5710 [M + H⁺].

(E)-1-(6-((4-(1-isopropyl-1H-pyrazol-4-yl)-5-methylpyrimidin-2-yl)amino)-3,4-dihydroisoquinolin-2(1H)-yl)-4-phenylbut-2-ene-1,4-dione (13z). ¹H NMR (400 MHz, DMSO-*d*₆): δ 9.31 (d, *J* = 2.2 Hz, 1H), 8.33 (s, 1H), 8.28 (s, 1H), 8.13–8.02 (m, 3H), 7.85–7.79 (m, 1H), 7.76 (d, *J* = 2.2 Hz, 1H), 7.74–7.68 (m, 1H), 7.64–7.50 (m, 4H), 7.15 (dd, *J* = 8.5, 4.3 Hz, 1H), 4.73 (d, *J* = 36.9 Hz, 2H), 4.63 (p, *J* = 6.7 Hz, 1H), 3.83 (dt, *J* = 11.2, 5.9 Hz, 2H), 2.88 (dt, *J* = 23.7, 6.0 Hz, 2H), 2.32 (s, 3H), 1.49 (dd, *J* = 6.7, 1.9 Hz, 6H). ¹³C NMR (101 MHz, DMSO): δ 188.40, 167.72, 157.94, 151.75, 138.93, 138.16, 132.71, 129.12, 125.20, 121.82, 120.43, 119.95, 117.79, 54.16, 47.73, 44.20, 29.77, 23.16, 15.47. HRMS (ESI) *m/z*: 507.6100 [M + H⁺].

(E)-1-(6-((4-(1-isopropyl-1H-pyrazol-4-yl)-5-methylpyrimidin-2-yl)amino)-3,4-dihydroisoquinolin-2(1H)-yl)-4-(*p*-tolyl)but-2-ene-1,4-dione (13aa). ¹H NMR (400 MHz, DMSO-*d*₆): δ 9.31 (d, *J* = 2.1 Hz, 1H), 8.33 (s, 1H), 8.28 (s, 1H), 8.09 (s, 1H), 7.96 (dd, *J* = 8.3, 2.8 Hz, 2H), 7.84–7.72 (m, 2H), 7.59–7.48 (m, 2H), 7.39 (d, *J* = 8.0 Hz, 2H), 7.14 (dd, *J* = 8.5, 3.8 Hz, 1H), 4.79–4.58 (m, 3H),

3.82 (dt, *J* = 10.1, 5.9 Hz, 2H), 2.88 (dt, *J* = 23.6, 6.0 Hz, 2H), 2.40 (s, 3H), 2.32 (s, 3H), 1.48 (dd, *J* = 6.7, 1.7 Hz, 6H). ¹³C NMR (101 MHz, DMSO): δ 189.47, 164.43, 164.20, 159.91, 158.92, 157.70, 144.87, 140.16, 140.04, 139.33, 135.04, 134.85, 134.59, 134.11, 133.90, 133.72, 130.06, 129.46, 129.31, 126.99, 126.82, 125.73, 125.62, 120.66, 118.21, 117.29, 117.17, 116.62, 53.84, 47.03, 44.33, 43.85, 29.88, 28.79, 23.04, 21.70, 17.16. HRMS (ESI) *m/z*: 521.6370 [M + H⁺].

1-(6-((4-(1-isopropyl-1H-pyrazol-4-yl)-5-methylpyrimidin-2-yl)amino)-3,4-dihydroisoquinolin-2(1H)-yl)-4-(*p*-tolyl)butane-1,4-dione (13ab). ¹H NMR (400 MHz, DMSO-*d*₆): δ 9.30 (d, *J* = 5.9 Hz, 1H), 8.31 (d, *J* = 20.9 Hz, 2H), 8.09 (d, *J* = 1.7 Hz, 1H), 7.88 (d, *J* = 8.0 Hz, 2H), 7.75 (dd, *J* = 11.7, 1.8 Hz, 1H), 7.61–7.51 (m, 1H), 7.33 (d, *J* = 7.8 Hz, 2H), 7.11 (dd, *J* = 25.0, 8.4 Hz, 1H), 4.71–4.49 (m, 3H), 3.71 (dt, *J* = 35.7, 5.9 Hz, 2H), 3.24 (t, *J* = 6.2 Hz, 2H), 2.95–2.71 (m, 4H), 2.35 (d, *J* = 24.3 Hz, 6H), 1.49 (d, *J* = 6.6 Hz, 6H). ¹³C NMR (101 MHz, DMSO-*d*₆): δ 198.87, 170.54, 170.46, 159.90, 158.95, 157.69, 143.72, 140.03, 139.92, 139.34, 135.26, 135.03, 134.80, 129.62, 129.44, 128.41, 126.84, 126.47, 125.93, 120.70, 118.31, 118.24, 117.19, 116.59, 116.56, 53.84, 46.43, 43.82, 43.09, 33.38, 29.66, 29.02, 27.73, 27.30, 23.03, 21.59, 17.16. HRMS (ESI) *m/z*: 523.6530 [M + H⁺].

(E)-4-(Dimethylamino)-1-(6-((4-(1-isopropyl-1H-pyrazol-4-yl)-5-methylpyrimidin-2-yl)amino)-3,4-dihydroisoquinolin-2(1H)-yl)but-2-en-1-one (13ac). ¹H NMR (400 MHz, DMSO-*d*₆): δ 9.30 (d, *J* = 5.2 Hz, 1H), 8.30 (d, *J* = 20.8 Hz, 2H), 8.09 (s, 1H), 7.75 (d, *J* = 6.4 Hz, 1H), 7.56 (t, *J* = 9.0 Hz, 1H), 7.10 (t, *J* = 8.8 Hz, 1H), 6.85 (d, *J* = 15.1 Hz, 1H), 6.70–6.56 (m, 1H), 4.71 (s, 1H), 4.65–4.57 (m, 2H), 3.77 (dt, *J* = 18.4, 5.8 Hz, 2H), 3.51 (d, *J* = 6.6 Hz, 2H), 2.84 (dt, *J* = 28.8, 6.0 Hz, 2H), 2.32 (s, 3H), 1.49 (d, *J* = 6.6 Hz, 6H). ¹³C NMR (101 MHz, DMSO): δ 164.68, 164.48, 159.88, 158.92, 157.67, 148.07, 140.10, 139.97, 139.46, 139.34, 139.22, 135.13, 134.82, 129.41, 127.95, 126.92, 126.65, 126.19, 125.84, 125.23, 120.69, 119.55, 118.33, 118.23, 117.26, 117.15, 116.59, 65.38, 59.54, 53.85, 44.57, 44.17, 43.46, 29.96, 23.01, 17.15. HRMS (ESI) *m/z*: 460.5980 [M + H⁺].

4-(Dimethylamino)-1-(6-((4-(1-isopropyl-1H-pyrazol-4-yl)-5-methylpyrimidin-2-yl)amino)-3,4-dihydroisoquinolin-2(1H)-yl)butan-1-one (13ad). ¹H NMR (400 MHz, DMSO-*d*₆): δ 9.30 (d, *J* = 6.4 Hz, 1H), 8.33 (s, 1H), 8.28 (s, 1H), 8.09 (s, 1H), 7.75 (dd, *J* = 10.1, 2.2 Hz, 1H), 7.56 (ddd, *J* = 14.8, 8.4, 2.2 Hz, 1H), 7.10 (d, *J* = 8.4 Hz, 1H), 4.68–4.54 (m, 3H), 3.68 (dt, *J* = 12.1, 5.9 Hz, 2H), 3.09–2.99 (m, 2H), 2.88 (s, 8H), 2.56–2.51 (m, 2H), 2.32 (s, 3H), 1.87 (p, *J* = 7.0 Hz, 2H), 1.48 (d, *J* = 6.6 Hz, 6H). ¹³C NMR (101 MHz, DMSO): δ 170.49, 170.41, 159.92, 158.92, 157.68, 140.07, 139.95, 139.34, 135.21, 134.95, 129.44, 126.88, 126.71, 126.30, 125.78, 120.66, 118.34, 118.21, 117.22, 116.66, 116.62, 57.26, 53.86, 46.45, 43.82, 43.07, 42.89, 30.17, 29.84, 29.58, 28.94, 23.02, 22.89, 20.15, 17.13. HRMS (ESI) *m/z*: 462.6140 [M + H⁺].

(E)-4-(6-((4-(1-isopropyl-1H-pyrazol-4-yl)-5-methylpyrimidin-2-yl)amino)-3,4-dihydroisoquinolin-2(1H)-yl)but-2-enoic Acid (13ae). ¹H NMR (400 MHz, DMSO-*d*₆): δ 9.21 (s, 1H), 8.30 (d, *J* = 22.4 Hz, 2H), 8.08 (s, 1H), 7.67 (d, *J* = 2.3 Hz, 1H), 7.48 (dd, *J* = 8.3, 2.2 Hz, 1H), 6.96 (d, *J* = 8.4 Hz, 1H), 6.79 (dt, *J* = 15.6, 5.9 Hz, 1H), 6.02–5.94 (m, 1H), 4.62 (h, *J* = 6.6 Hz, 1H), 3.51 (s, 2H), 3.27 (d, *J* = 5.5 Hz, 2H), 3.18 (s, 1H), 2.83 (t, *J* = 5.8 Hz, 2H), 2.67 (t, *J* = 5.8 Hz, 2H), 2.31 (s, 3H), 1.49 (d, *J* = 6.6 Hz, 6H). ¹³C NMR (101 MHz, DMSO-*d*₆): δ 170.53, 158.50, 157.32, 152.38, 144.77, 138.89, 133.26, 129.05, 125.84, 125.17, 122.18, 120.54, 119.69, 119.22, 117.89, 56.52, 55.36, 54.11, 50.45, 28.84, 23.16, 15.48. HRMS (ESI) *m/z*: 433.5680 [M + H⁺].

(E)-4-(6-((4-(1-isopropyl-1H-pyrazol-4-yl)-5-methylpyrimidin-2-yl)amino)-3,4-dihydroisoquinolin-2(1H)-yl)-N-(2-(piperidin-1-yl)ethyl)but-2-enamide (13af). ¹H NMR (400 MHz, DMSO-*d*₆): δ 9.22 (s, 1H), 8.33 (s, 1H), 8.27 (s, 1H), 8.09 (s, 2H), 7.68 (d, *J* = 2.2 Hz, 1H), 7.48 (dd, *J* = 8.3, 2.2 Hz, 1H), 6.96 (d, *J* = 8.3 Hz, 1H), 6.67 (dt, *J* = 15.4, 5.9 Hz, 1H), 6.14 (d, *J* = 15.5 Hz, 1H), 4.62 (h, *J* = 6.6 Hz, 1H), 3.53 (s, 2H), 3.29–3.21 (m, 3H), 2.87–2.81 (m, 2H), 2.69 (d, *J* = 8.0 Hz, 2H), 2.32 (s, 3H), 1.49 (d, *J* = 6.6 Hz, 12H). ¹³C NMR (101 MHz, DMSO-*d*₆): δ 167.03, 157.94, 157.26, 151.81, 141.33, 138.80, 138.62, 134.04, 128.44, 125.75, 125.22, 122.48, 120.43, 120.19, 120.13, 117.84, 56.00, 55.63, 54.14, 53.65, 50.44, 38.81, 28.20, 26.43, 23.84, 23.16, 15.43. HRMS (ESI) *m/z*: 543.7320 [M + H⁺].

(*E*)-*N*-(*tert*-Butyl)-4-(6-((4-(1-isopropyl-1*H*-pyrazol-4-yl)-5-methylpyrimidin-2-yl)amino)-3,4-dihydroisoquinolin-2(1*H*)-yl)but-2-enamide (**13ag**). ¹H NMR (400 MHz, DMSO-*d*₆): δ 9.21 (s, 1H), 8.30 (d, *J* = 22.0 Hz, 2H), 8.09 (s, 1H), 7.71–7.56 (m, 2H), 7.48 (dd, *J* = 8.3, 2.2 Hz, 1H), 6.96 (d, *J* = 8.4 Hz, 1H), 6.58 (dt, *J* = 15.4, 5.9 Hz, 1H), 6.15 (dd, *J* = 15.4, 1.6 Hz, 1H), 4.63 (p, *J* = 6.6 Hz, 1H), 3.50 (s, 2H), 3.26–3.15 (m, 2H), 2.84 (t, *J* = 5.8 Hz, 2H), 2.66 (t, *J* = 5.8 Hz, 2H), 2.32 (s, 3H), 1.49 (d, *J* = 6.6 Hz, 6H), 1.29 (s, 9H). ¹³C NMR (101 MHz, DMSO): δ 164.52, 159.90, 158.99, 157.65, 139.53, 139.31, 138.56, 134.34, 129.41, 127.68, 127.63, 126.77, 120.71, 118.32, 116.76, 116.39, 58.83, 55.77, 53.83, 51.06, 50.47, 29.59, 29.03, 23.05, 17.15. HRMS (ESI) *m/z*: 488.6520 [M + H⁺].

(*E*)-*N,N*-Diethyl-4-(6-((4-(1-isopropyl-1*H*-pyrazol-4-yl)-5-methylpyrimidin-2-yl)amino)-3,4-dihydroisoquinolin-2(1*H*)-yl)but-2-enamide (**13ah**). ¹H NMR (400 MHz, DMSO-*d*₆): δ 9.21 (s, 1H), 8.30 (d, *J* = 22.5 Hz, 2H), 8.08 (s, 1H), 7.67 (d, *J* = 2.2 Hz, 1H), 7.48 (dd, *J* = 8.4, 2.2 Hz, 1H), 6.96 (d, *J* = 8.4 Hz, 1H), 6.71 (dt, *J* = 15.1, 6.0 Hz, 1H), 6.61–6.52 (m, 1H), 4.63 (hept, *J* = 6.7 Hz, 1H), 3.52 (s, 2H), 3.38 (s, 3H), 3.30–3.25 (m, 2H), 2.83 (t, *J* = 5.9 Hz, 2H), 2.68 (t, *J* = 5.8 Hz, 2H), 2.32 (s, 3H), 1.49 (d, *J* = 6.7 Hz, 6H), 1.17–0.99 (m, 7H). ¹³C NMR (101 MHz, DMSO): δ 159.85, 158.70, 157.79, 154.11, 139.32, 137.19, 137.08, 129.48, 120.53, 120.22, 116.78, 114.55, 106.91, 63.14, 53.84, 48.24, 35.15, 33.95, 23.05, 18.71, 17.15, 11.35. HRMS (ESI) *m/z*: 488.6542 [M + H⁺].

2-(7-((4-(1-isopropyl-1*H*-pyrazol-4-yl)-5-methylpyrimidin-2-yl)amino)-3,4-dihydroisoquinolin-2(1*H*)-yl)acetonitrile (**13ai**). ¹H NMR (400 MHz, DMSO-*d*₆): δ 9.25 (s, 1H), 8.30 (d, *J* = 21.5 Hz, 2H), 8.09 (s, 1H), 7.65 (d, *J* = 2.3 Hz, 1H), 7.50 (dd, *J* = 8.3, 2.2 Hz, 1H), 7.04 (d, *J* = 8.4 Hz, 1H), 4.63 (hept, *J* = 6.7 Hz, 1H), 3.93 (s, 2H), 3.68 (s, 2H), 2.84–2.71 (m, 4H), 2.32 (s, 3H), 1.49 (d, *J* = 6.6 Hz, 6H). ¹³C NMR (101 MHz, DMSO): δ 159.90, 158.96, 157.66, 139.32, 139.29, 133.95, 133.95, 129.38, 128.93, 125.94, 120.72, 117.55, 116.47, 116.34, 116.20, 54.40, 53.85, 49.90, 45.51, 40.00, 28.39, 23.04, 17.16. HRMS (ESI) *m/z*: 388.4910 [M + H⁺].

(*E*)-1-(7-((4-(1-isopropyl-1*H*-pyrazol-4-yl)-5-methylpyrimidin-2-yl)amino)-3,4-dihydroisoquinolin-2(1*H*)-yl)-4-phenylbut-2-ene-1,4-dione (**13aj**). ¹H NMR (400 MHz, DMSO-*d*₆): δ 9.31 (d, *J* = 3.6 Hz, 1H), 8.34 (s, 1H), 8.28 (d, *J* = 7.3 Hz, 1H), 8.12–8.01 (m, 3H), 7.85–7.75 (m, 2H), 7.73–7.67 (m, 1H), 7.62–7.50 (m, 4H), 7.10 (d, *J* = 8.3 Hz, 1H), 4.79 (d, *J* = 40.6 Hz, 2H), 4.61 (dq, *J* = 13.3, 6.7 Hz, 1H), 3.82 (dt, *J* = 10.9, 5.9 Hz, 2H), 2.82 (dt, *J* = 24.6, 5.9 Hz, 2H), 2.32 (d, *J* = 4.6 Hz, 3H), 1.48 (dd, *J* = 16.7, 6.6 Hz, 6H). ¹³C NMR (101 MHz, DMSO): δ 188.48, 167.69, 157.94, 151.81, 138.93, 138.61, 138.16, 132.55, 132.01, 131.74, 130.78, 128.97, 127.02, 125.22, 121.82, 119.95, 118.78, 54.13, 46.66, 44.21, 29.07, 23.19, 15.44. HRMS (ESI) *m/z*: 507.6100 [M + H⁺].

Methyl-(*E*)-4-(7-((4-(1-isopropyl-1*H*-pyrazol-4-yl)-5-methylpyrimidin-2-yl)amino)-3,4-dihydroisoquinolin-2(1*H*)-yl)but-2-enoate (**13ak**). ¹H NMR (400 MHz, DMSO-*d*₆): δ 9.21 (s, 1H), 8.32 (s, 1H), 8.26 (d, *J* = 5.5 Hz, 1H), 8.07 (d, *J* = 6.0 Hz, 1H), 7.61 (s, 1H), 7.50–7.45 (m, 1H), 7.00 (t, *J* = 9.9 Hz, 1H), 6.93 (dt, *J* = 15.7, 5.8 Hz, 1H), 6.10 (d, *J* = 15.7 Hz, 1H), 4.62 (dt, *J* = 13.3, 6.6 Hz, 1H), 3.68 (s, 3H), 3.58 (s, 2H), 3.32–3.29 (m, 2H), 2.75 (d, *J* = 5.1 Hz, 2H), 2.67 (t, *J* = 5.4 Hz, 2H), 2.30 (d, *J* = 9.3 Hz, 3H), 1.48 (d, *J* = 6.7 Hz, 6H). ¹³C NMR (101 MHz, DMSO): δ 166.38, 159.89, 158.97, 157.64, 146.65, 139.26, 139.16, 134.82, 129.36, 128.84, 126.72, 122.54, 120.75, 117.36, 116.39, 116.26, 65.38, 58.42, 56.33, 53.83, 51.81, 51.08, 28.45, 23.02, 17.14, 15.62. HRMS (ESI) *m/z*: 447.5550 [M + H⁺].

(*E*)-1-(7-((4-(1-isopropyl-1*H*-pyrazol-4-yl)-5-methylpyrimidin-2-yl)amino)-3,4-dihydroisoquinolin-2(1*H*)-yl)-4-(*p*-tolyl)but-2-ene-1,4-dione (**13al**). ¹H NMR (400 MHz, DMSO-*d*₆): δ 9.31 (d, *J* = 3.4 Hz, 1H), 8.39–8.21 (m, 2H), 8.08 (d, *J* = 10.4 Hz, 1H), 7.96 (dd, *J* = 8.0, 4.3 Hz, 2H), 7.88–7.68 (m, 2H), 7.61–7.47 (m, 2H), 7.38 (dd, *J* = 8.1, 4.2 Hz, 2H), 7.10 (d, *J* = 8.3 Hz, 1H), 4.94–4.49 (m, 3H), 3.82 (dt, *J* = 9.7, 5.9 Hz, 2H), 2.81 (dt, *J* = 24.2, 5.9 Hz, 2H), 2.40 (d, *J* = 3.7 Hz, 3H), 2.32 (d, *J* = 4.5 Hz, 3H), 1.48 (dd, *J* = 16.3, 6.7 Hz, 6H). ¹³C NMR (101 MHz, DMSO): δ 188.51, 167.69, 157.92, 151.75, 142.36, 138.67, 136.61, 131.44, 130.18, 129.22, 128.97, 126.98, 125.22, 121.82, 119.95, 118.51, 54.14, 46.66, 44.23, 29.07, 23.16, 21.34, 15.44. HRMS (ESI) *m/z*: 521.6370 [M + H⁺].

(*E*)-4-(Dimethylamino)-1-(7-((4-(1-isopropyl-1*H*-pyrazol-4-yl)-5-methylpyrimidin-2-yl)amino)-3,4-dihydroisoquinolin-2(1*H*)-yl)but-2-en-1-one (**13am**). ¹H NMR (400 MHz, DMSO-*d*₆): δ 9.32 (d, *J* = 10.3 Hz, 1H), 8.34 (d, *J* = 5.4 Hz, 1H), 8.28 (s, 1H), 8.10 (s, 1H), 7.76 (d, *J* = 13.3 Hz, 1H), 7.54 (dd, *J* = 8.3, 2.3 Hz, 1H), 7.10 (d, *J* = 8.4 Hz, 1H), 6.95 (dd, *J* = 23.4, 15.0 Hz, 1H), 6.65 (dt, *J* = 14.7, 6.8 Hz, 1H), 4.79 (s, 1H), 4.69 (s, 1H), 4.63 (q, *J* = 6.7 Hz, 1H), 3.79 (dt, *J* = 15.3, 5.9 Hz, 2H), 3.68 (d, *J* = 6.9 Hz, 2H), 2.79 (dt, *J* = 30.7, 5.8 Hz, 2H), 2.63 (s, 6H), 2.32 (s, 3H), 1.50 (d, *J* = 6.7 Hz, 6H). ¹³C NMR (101 MHz, DMSO): δ 166.48, 157.98, 157.32, 151.95, 139.51, 138.89, 138.61, 131.22, 130.08, 126.99, 125.17, 122.18, 119.89, 119.75, 118.46, 58.03, 54.16, 46.57, 45.19, 44.61, 29.28, 23.19, 15.48. HRMS (ESI) *m/z*: 460.5988 [M + H⁺].

ASSOCIATED CONTENT

Supporting Information

The Supporting Information is available free of charge at <https://pubs.acs.org/doi/10.1021/acs.jmedchem.0c01488>.

Binding affinities of **13ac** with 365 protein kinases; ¹H NMR, ¹³C NMR, MS/MS, and HPLC spectra of compound **13ac**; routine blood test in normal mice; and effect of **13ac** on mouse models (PDF)

PDB code 2XA4 used for modeling docking in JAK2 of **13ac** (PDB)

PDB code: 4RT7 used for modeling docking in FLT3 of **18e** (PDB)

Molecular formula strings of the prepared compounds (CSV)

AUTHOR INFORMATION

Corresponding Authors

Zhuang Yang — State Key Laboratory of Biotherapy and Cancer Center, National Clinical Research Center for Geriatrics, West China Hospital of Sichuan University, Chengdu 610041, China; Chengdu Zenitar Biomedical Technology Co., Ltd., Chengdu 610041, China; Email: young9008@126.com

Lijuan Chen — State Key Laboratory of Biotherapy and Cancer Center, National Clinical Research Center for Geriatrics, West China Hospital of Sichuan University, Chengdu 610041, China; Chengdu Zenitar Biomedical Technology Co., Ltd., Chengdu 610041, China; orcid.org/0000-0002-8076-163X; Phone: +86-28-85164063; Email: chenlijuan125@163.com

Authors

Tao Yang — State Key Laboratory of Biotherapy and Cancer Center, National Clinical Research Center for Geriatrics, West China Hospital of Sichuan University, Chengdu 610041, China

Mengshi Hu — State Key Laboratory of Biotherapy and Cancer Center, National Clinical Research Center for Geriatrics, West China Hospital of Sichuan University, Chengdu 610041, China

Yong Chen — State Key Laboratory of Biotherapy and Cancer Center, National Clinical Research Center for Geriatrics, West China Hospital of Sichuan University, Chengdu 610041, China

Mingli Xiang — State Key Laboratory of Biotherapy and Cancer Center, National Clinical Research Center for Geriatrics, West China Hospital of Sichuan University, Chengdu 610041, China

Minghai Tang — State Key Laboratory of Biotherapy and Cancer Center, National Clinical Research Center for

Geriatrics, West China Hospital of Sichuan University, Chengdu 610041, China

Wenyan Qi – State Key Laboratory of Biotherapy and Cancer Center, National Clinical Research Center for Geriatrics, West China Hospital of Sichuan University, Chengdu 610041, China

Mingsong Shi – State Key Laboratory of Biotherapy and Cancer Center, National Clinical Research Center for Geriatrics, West China Hospital of Sichuan University, Chengdu 610041, China

Jun He – State Key Laboratory of Biotherapy and Cancer Center, National Clinical Research Center for Geriatrics, West China Hospital of Sichuan University, Chengdu 610041, China

Xue Yuan – State Key Laboratory of Biotherapy and Cancer Center, National Clinical Research Center for Geriatrics, West China Hospital of Sichuan University, Chengdu 610041, China

Chufeng Zhang – State Key Laboratory of Biotherapy and Cancer Center, National Clinical Research Center for Geriatrics, West China Hospital of Sichuan University, Chengdu 610041, China

Kongjun Liu – State Key Laboratory of Biotherapy and Cancer Center, National Clinical Research Center for Geriatrics, West China Hospital of Sichuan University, Chengdu 610041, China

Jiwen Li – State Key Laboratory of Biotherapy and Cancer Center, National Clinical Research Center for Geriatrics, West China Hospital of Sichuan University, Chengdu 610041, China

Complete contact information is available at:
<https://pubs.acs.org/10.1021/acs.jmedchem.0c01488>

Author Contributions

[§]T.Y., M.H., and Y.C. contributed equally and should be considered as co-first authors

Notes

The authors declare no competing financial interest.

ACKNOWLEDGMENTS

The authors greatly appreciate the financial support from the National Science Foundation of China (81527806, 82073693, and 81673289) and Post-Doctor Research Project, West China Hospital, Sichuan University (2018HXBH054). The authors also greatly appreciate the financial support from 1.3.5 project for disciplines of excellence, West China Hospital, Sichuan University. Thanks to West China College of Pharmacy Sichuan University for providing Schrodinger software and technical support.

ABBREVIATIONS

JAK1, Janus kinase 1; JAK2, Janus kinase 2; JAK3, Janus kinase 3; TFA, trifluoroacetic acid; TLC, thin layer chromatography; MTT, 3-(4,5-dimethylthiazol-2-yl)-2,5-diphenyltetrazolium bromide; PE, petroleum ether; EA, ethyl acetate; DCM, dichloromethane

REFERENCES

- (1) Spivak, J. L. Myeloproliferative neoplasms. *N. Engl. J. Med.* **2017**, *376*, 2168–2181.
- (2) Nangalia, J.; Green, A. R. Myeloproliferative neoplasms: from origins to outcomes. *Blood* **2017**, *130*, 2475–2483.

- (3) Arber, D. A.; Orazi, A.; Hasserjian, R.; Thiele, J.; Borowitz, M. J.; Le Beau, M. M.; Bloomfield, C. D.; Cazzola, M.; Vardiman, J. W. The 2016 revision to the World Health Organization classification of myeloid neoplasms and acute leukemia. *Blood* **2016**, *127*, 2391–2405.

- (4) Tefferi, A.; Pardanani, A. Myeloproliferative neoplasms: a contemporary review. *JAMA. Oncol.* **2015**, *1*, 97–105.

- (5) Pardanani, A.; Gotlib, J.; Roberts, A. W.; Wadleigh, M.; Sirhan, S.; Kawashima, J.; Maltzman, J. A.; Shao, L.; Gupta, V.; Tefferi, A. Long-term efficacy and safety of momelotinib, a JAK1 and JAK2 inhibitor, for the treatment of myelofibrosis. *Leukemia* **2018**, *32*, 1035–1038.

- (6) Verstovsek, S.; Kantarjian, H. M.; Estrov, Z.; Cortes, J. E.; Thomas, D. A.; Kadia, T.; Pierce, S.; Jabbour, E.; Borthakur, G.; Rumi, E.; Pungolino, E.; Morra, E.; Caramazza, D.; Cazzola, M.; Passamonti, F. Long-term outcomes of 107 patients with myelofibrosis receiving JAK1/JAK2 inhibitor ruxolitinib: survival advantage in comparison to matched historical controls. *Blood* **2012**, *120*, 1202–1209.

- (7) Levine, R. L.; Pardanani, A.; Tefferi, A.; Gilliland, D. G. Role of JAK2 in the pathogenesis and therapy of myeloproliferative disorders. *Nat. Rev. Cancer* **2007**, *7*, 673–683.

- (8) Passamonti, F.; Maffioli, M. The role of JAK2 inhibitors in MPNs 7 years after approval. *Blood* **2018**, *131*, 2426–2435.

- (9) Levine, R. L.; Wadleigh, M.; Coombs, J.; Ebert, B. L.; Wernig, G.; Huntly, B. J. P.; Boggon, T. J.; Wlodarska, I.; Clark, J. J.; Moore, S.; Adelsperger, J.; Koo, S.; Lee, J. C.; Gabriel, S.; Mercher, T.; D'Andrea, A.; Fröhling, S.; Döhner, K.; Marynen, P.; Vandenberghe, P.; Mesa, R. A.; Tefferi, A.; Griffin, J. D.; Eck, M. J.; Sellers, W. R.; Meyerson, M.; Golub, T. R.; Lee, S. J.; Gilliland, D. G. Activating mutation in the tyrosine kinase JAK2 in polycythemia vera, essential thrombocythemia, and myeloid metaplasia with myelofibrosis. *Cancer Cell* **2005**, *7*, 387–397.

- (10) Perner, F.; Perner, C.; Ernst, T.; Heide, F. H. Roles of JAK2 in aging, inflammation, hematopoiesis and malignant transformation. *Cells* **2019**, *8*, 854.

- (11) Boissinot, M.; Cleyrat, C.; Vilaine, M.; Jacques, Y.; Corre, I.; Hermouet, S. Anti-inflammatory cytokines hepatocyte growth factor and interleukin-11 are over-expressed in polycythemia vera and contribute to the growth of clonal erythroblasts independently of JAK2V617F. *Oncogene* **2011**, *30*, 990–1001.

- (12) Dupont, S.; Massé, A.; James, C.; Teyssandier, I.; Lécluse, Y.; Larbret, F.; Ugo, V.; Saulnier, P.; Koscielny, S.; Le Couédic, J. P.; Casadevall, N.; Vainchenker, W.; Delhommeau, F. The JAK2 617V>F mutation triggers erythropoietin hypersensitivity and terminal erythroid amplification in primary cells from patients with polycythemia vera. *Blood* **2007**, *110*, 1013–1021.

- (13) Jang, Y.-N.; Baik, E. J. JAK-STAT pathway and myogenic differentiation. *JAK-STAT* **2013**, *2*, e23282.

- (14) James, C.; Ugo, V.; Le Couédic, J.-P.; Staerk, J.; Delhommeau, F.; Lacout, C.; Garçon, L.; Raslova, H.; Berger, R.; Bennaceur-GrisCELLI, A.; Villeval, J. L.; Constantinescu, S. N.; Casadevall, N.; Vainchenker, W. A unique clonal JAK2 mutation leading to constitutive signalling causes polycythemia vera. *Nature* **2005**, *434*, 1144–1148.

- (15) Vannucchi, A. M.; Kiladjian, J. J.; Griesshammer, M.; Masszi, T.; Durrant, S.; Passamonti, F.; Harrison, C. N.; Pane, F.; Zachee, P.; Mesa, R.; He, S.; Jones, M. M.; Garrett, W.; Li, J.; Pirron, U.; Habr, D.; Verstovsek, S. Ruxolitinib versus standard therapy for the treatment of polycythemia vera. *N. Engl. J. Med.* **2015**, *372*, 426–435.

- (16) Blair, H. A. Fedratinib: first approval. *Drugs* **2019**, *79*, 1719–1725.

- (17) Hexner, E. O.; Serdikoff, C.; Jan, M.; Swider, C. R.; Robinson, C.; Yang, S.; Angeles, T.; Emerson, S. G.; Carroll, M.; Ruggeri, B.; Dobrzanski, P. Lestaurtinib (CEP701) is a JAK2 inhibitor that suppresses JAK2/STAT5 signaling and the proliferation of primary erythroid cells from patients with myeloproliferative disorders. *Blood* **2008**, *111*, 5663–5671.

- (18) Tyner, J. W.; Bumm, T. G.; Deininger, J.; Wood, L.; Aichberger, K. J.; Loriaux, M. M.; Druker, B. J.; Burns, C. J.; Fantino, E.; Deininger, M. W. CYT387, a novel JAK2 inhibitor, induces hematologic responses and normalizes inflammatory cytokines in murine myeloproliferative neoplasms. *Blood* **2010**, *115*, 5232–5240.

- (19) Harrison, C. N.; Vannucchi, A. M.; Platzbecker, U.; Cervantes, F.; Gupta, V.; Lavie, D.; Passamonti, F.; Winton, E. F.; Dong, H.; Kawashima, J.; Maltzman, J. D.; Kiladjian, J.-J.; Verstovsek, S. Momelotinib versus best available therapy in patients with myelofibrosis previously treated with ruxolitinib (SIMPLIFY 2): a randomised, open-label, phase 3 trial. *Lancet Haematol.* **2018**, *5*, e73–e81.
- (20) Berdeja, J.; Palandri, F.; Baer, M. R.; Quick, D.; Kiladjian, J. J.; Martinelli, G.; Verma, A.; Hamid, O.; Walgren, R.; Pitou, C.; Li, P. L.; Gerds, A. T. Phase 2 study of gandotinib (LY2784544) in patients with myeloproliferative neoplasms. *Leuk. Res.* **2018**, *71*, 82–88.
- (21) Mascarenhas, J.; Hoffman, R.; Talpaz, M.; Gerds, A. T.; Stein, B.; Gupta, V.; Szoke, A.; Drummond, M.; Pristupa, A.; Granston, T.; Daly, R.; Al-Fayoumi, S.; Callahan, J. A.; Singer, J. W.; Gotlib, J.; Jamieson, C.; Harrison, C.; Mesa, R.; Verstovsek, S. Pacritinib vs best available therapy, including ruxolitinib, in patients with myelofibrosis: a randomized clinical trial. *JAMA. Oncol.* **2018**, *4*, 652–659.
- (22) Pardanani, A.; Harrison, C.; Cortes, J. E.; Cervantes, F.; Mesa, R. A.; Milligan, D.; Masszi, T.; Mischchenko, E.; Jourdan, E.; Vannucchi, A. M.; Drummond, M. W.; Jurgutis, M.; Kuliczowski, K.; Gheorghita, E.; Passamonti, F.; Neumann, F.; Patki, A.; Gao, G.; Tefferi, A. Safety and efficacy of fedratinib in patients with primary or secondary myelofibrosis: a randomized clinical trial. *JAMA. Oncol.* **2015**, *1*, 643–651.
- (23) Mullally, A.; Hood, J.; Harrison, C.; Mesa, R. Fedratinib in myelofibrosis. *Blood Adv.* **2020**, *4*, 1792–1800.
- (24) Wan, H.; Schroeder, G. M.; Hart, A. C.; Inghrim, J.; Grebinski, J.; Tokarski, J. S.; Lorenzi, M. V.; You, D.; McDevitt, T.; Penhallow, B.; Vuppugalla, R.; Zhang, Y.; Gu, X.; Iyer, R.; Lombardo, L. J.; Trainor, G. L.; Ruepp, S.; Lippy, J.; Blat, Y.; Sack, J. S.; Khan, J. A.; Stefanski, K.; Slecicka, B.; Mathur, A.; Sun, J.-H.; Wong, M. K.; Wu, D.-R.; Li, P.; Gupta, A.; Arunachalam, P. N.; Pragalathan, B.; Narayanan, S.; Nanjundaswamy, K. C.; Kuppusamy, P.; Purandare, A. V. Discovery of a highly selective JAK2 inhibitor, BMS-911543, for the treatment of myeloproliferative neoplasms. *ACS. Med. Chem. Lett.* **2015**, *6*, 850–855.
- (25) Yang, T.; Hu, M.; Qi, W.; Yang, Z.; Tang, M.; He, J.; Chen, Y.; Bai, P.; Yuan, X.; Zhang, C.; Liu, K.; Lu, Y.; Xiang, M.; Chen, L. Discovery of potent and orally effective dual janus kinase 2/FLT3 inhibitors for the treatment of acute myelogenous leukemia and myeloproliferative neoplasms. *J. Med. Chem.* **2019**, *62*, 10305–10320.
- (26) Engelhardt, H.; Böse, D.; Petronczki, M.; Scharn, D.; Bader, G.; Baum, A.; Bergner, A.; Chong, E.; Döbel, S.; Egger, G.; Engelhardt, C.; Ettmayer, P.; Fuchs, J. E.; Gerstberger, T.; Gonnella, N.; Grimm, A.; Grondal, E.; Haddad, N.; Hopfgartner, B.; Kousek, R.; Krawiec, M.; Kriz, M.; Lamarre, L.; Leung, J.; Mayer, M.; Patel, N. D.; Simov, B. P.; Reeves, J. T.; Schnitzer, R.; Schrenk, A.; Sharps, B.; Solca, F.; Stadtmüller, H.; Tan, Z.; Wunberg, T.; Zoephel, A.; McConnell, D. B. Start selective and rigidify: the discovery path toward a next generation of EGFR tyrosine kinase inhibitors. *J. Med. Chem.* **2019**, *62*, 10272–10293.
- (27) Drilon, A.; Nagasubramanian, R.; Blake, J. F.; Ku, N.; Tuch, B. B.; Ebata, K.; Smith, S.; Lauriault, V.; Kolakowski, G. R.; Brandhuber, B. J.; Larsen, P. D.; Bouhana, K. S.; Winski, S. L.; Hamor, R.; Wu, W.-L.; Parker, A.; Morales, T. H.; Sullivan, F. X.; DeWolf, W. E.; Wollenberg, L. A.; Gordon, P. R.; Douglas-Lindsay, D. N.; Scaltriti, M.; Benayed, R.; Raj, S.; Hanusch, B.; Schram, A. M.; Jonsson, P.; Berger, M. F.; Hechtman, J. F.; Taylor, B. S.; Andrews, S.; Rothenberg, S. M.; Hyman, D. M. A next-generation TRK kinase inhibitor overcomes acquired resistance to prior TRK kinase inhibition in patients with TRK fusion-positive solid tumors. *Canc. Discov.* **2017**, *7*, 963–972.
- (28) Drilon, A.; Ou, S.-H. I.; Cho, B. C.; Kim, D.-W.; Lee, J.; Lin, J. J.; Zhu, V. W.; Ahn, M.-J.; Camidge, D. R.; Nguyen, J.; Zhai, D.; Deng, W.; Huang, Z.; Rogers, E.; Liu, J.; Whitten, J.; Lim, J. K.; Stopatschinskaja, S.; Hyman, D. M.; Doebele, R. C.; Cui, J. J.; Shaw, A. T. Repotrectinib (TPX-0005) is a next-generation ROS1/TRK/ALK inhibitor that potently inhibits ROS1/TRK/ALK solvent-front mutations. *Canc. Discov.* **2018**, *8*, 1227–1236.
- (29) Yamaura, T.; Nakatani, T.; Uda, K.; Ogura, H.; Shin, W.; Kurokawa, N.; Saito, K.; Fujikawa, N.; Date, T.; Takasaki, M.; Terada, D.; Hirai, A.; Akashi, A.; Chen, F.; Adachi, Y.; Ishikawa, Y.; Hayakawa, F.; Hagiwara, S.; Naoe, T.; Kiyoi, H. A novel irreversible FLT3 inhibitor, FF-10101, shows excellent efficacy against AML cells with FLT3 mutations. *Blood* **2018**, *131*, 426–438.
- (30) Barraco, F.; Greil, R.; Herbrecht, R.; Schmidt, B.; Reiter, A.; Willenbacher, W.; Raymakers, R.; Liersch, R.; Wroclawska, M.; Pack, R.; Burock, K.; Karumanchi, D.; Gisslinger, H. Real-world non-interventional long-term post-authorisation safety study of ruxolitinib in myelofibrosis. *Br. J. Haematol.* **2020**, DOI: 10.1111/bjh.16729.
- (31) Harrison, C. N.; Schaap, N.; Vannucchi, A. M.; Kiladjian, J.-J.; Tiu, R. V.; Zachee, P.; Jourdan, E.; Winton, E.; Silver, R. T.; Schouten, H. C.; Passamonti, F.; Zweegman, S.; Talpaz, M.; Lager, J.; Shun, Z.; Mesa, R. A. Janus kinase-2 inhibitor fedratinib in patients with myelofibrosis previously treated with ruxolitinib (JAKARTA-2): a single-arm, open-label, non-randomised, phase 2, multicentre study. *Lancet Haematol.* **2017**, *4*, e317–e324.
- (32) Brodeur, G. M.; Minturn, J. E.; Ho, R.; Simpson, A. M.; Iyer, R.; Varela, C. R.; Light, J. E.; Kolla, V.; Evans, A. E. Trk receptor expression and inhibition in neuroblastomas. *Clin. Cancer Res.* **2009**, *15*, 3244–3250.
- (33) Khotskaya, Y. B.; Holla, V. R.; Farago, A. F.; Mills Shaw, K. R.; Meric-Bernstam, F.; Hong, D. S. Targeting TRK family proteins in cancer. *Pharmacol. Ther.* **2017**, *173*, 58–66.
- (34) Mascarenhas, J.; Lu, M.; Li, T.; Petersen, B.; Hochman, T.; Najfeld, V.; Goldberg, J. D.; Hoffman, R. A phase I study of panobinostat (LBH589) in patients with primary myelofibrosis (PMF) and post-polycythaemia vera/essential thrombocythaemia myelofibrosis (post-PV/ET MF). *Br. J. Haematol.* **2013**, *161*, 68–75.
- (35) Berman, H. M.; Battistuz, T.; Bhat, T. N.; Bluhm, W. F.; Bourne, P. E.; Burkhardt, K.; Feng, Z.; Gilliland, G. L.; Iype, L.; Jain, S.; Fagan, P.; Marvin, J.; Padilla, D.; Ravichandran, V.; Schneider, B.; Thanki, N.; Weissig, H.; Westbrook, J. D.; Zardecki, C. The protein data bank. *Acta Crystallogr., Sect. D: Biol. Crystallogr.* **2002**, *58*, 899–907.
- (36) Ioannidis, S.; Lamb, M. L.; Wang, T.; Almeida, L.; Block, M. H.; Davies, A. M.; Peng, B.; Su, M.; Zhang, H.-J.; Hoffmann, E.; Rivard, C.; Green, I.; Howard, T.; Pollard, H.; Read, J.; Alimzhanov, M.; Bebernitiz, G.; Bell, K.; Ye, M.; Huszar, D.; Zinda, M. Discovery of 5-chloro-N2-[(1S)-1-(5-fluoropyrimidin-2-yl)ethyl]-N4-(5-methyl-1H-pyrazol-3-yl)pyrimidine-2,4-diamine (AZD1480) as a novel inhibitor of the Jak/Stat pathway. *J. Med. Chem.* **2011**, *54*, 262–276.
- (37) Sanner, M. F. Python: a programming language for software integration and development. *J. Mol. Graphics Modell.* **1999**, *17*, 57–61.
- (38) O’Boyle, N. M.; Banck, M.; James, C. A.; Morley, C.; Vandermeersch, T.; Hutchison, G. R. Open Babel: An open chemical toolbox. *J. Cheminf* **2011**, *3*, 33.
- (39) Morris, G. M.; Huey, R.; Lindstrom, W.; Sanner, M. F.; Belew, R. K.; Goodsell, D. S.; Olson, A. J. AutoDock4 and AutoDockTools4: Automated docking with selective receptor flexibility. *J. Comput. Chem.* **2009**, *30*, 2785–2791.
- (40) Fuhrmann, J.; Rurainski, A.; Lenhof, H. P.; Neumann, D. A new Lamarckian genetic algorithm for flexible ligand-receptor docking. *J. Comput. Chem.* **2010**, *31*, 1911–1918.
- (41) Gasteiger, J.; Marsili, M. Iterative partial equalization of orbital electronegativity—a rapid access to atomic charges. *Tetrahedron* **1980**, *36*, 3219–3228.
- (42) Stewart, J. J. P. Optimization of parameters for semiempirical methods I. method. *J. Comput. Chem.* **1989**, *10*, 209–220.